On Modelling the Atmospheres of Potentially-Habitable Super-Earths

ON MODELLING THE ATMOSPHERES OF POTENTIALLY-HABITABLE SUPER-EARTHS

BY

SARAH MCKENZIE-PICOT, B.Eng

A THESIS

SUBMITTED TO THE DEPARTMENT OF PHYSICS & ASTRONOMY

AND THE SCHOOL OF GRADUATE STUDIES

OF MCMASTER UNIVERSITY

IN PARTIAL FULFILMENT OF THE REQUIREMENTS

FOR THE DEGREE OF

MASTER OF SCIENCE

Master of Applied Science (2017)	McMaster University
(Physics & Astronomy)	Hamilton, Ontario, Canada

TITLE:	On Modelling the Atmospheres of Potentially-Habitable Super-Earths
AUTHOR:	Sarah McKenzie-Picot B.Eng., (Aerospace Engineering) Carleton University, Ottawa, Canada
SUPERVISOR:	Dr. Ralph Pudritz
NUMBER OF PAGES:	xiii, 88

Abstract

Atmospheres play an important role in the habitability of a planet, so understanding and modelling them is an important step in the search for life on other planets.

This thesis presents a 1D frequency-dependent radiative-convective code that was written to help determine the temperature-pressure structure of potentially-habitable exoplanets. This code pairs with a chemistry model to determine the chemical composition of these planets' atmospheres.

This code is applied to the planets in the TRAPPIST-1 system. The initial atmospheric compositions of the TRAPPIST-1 planets are determined through planet formation history and considered for both outgassed and accreted atmospheres. An interesting result is found when running these initial atmospheric compositions through the chemistry model: when the atmosphere equilibrates, it can change its C/O ratio from equal to that found in the accreted or outgassed volatiles to something lower, because, in temperate conditions, CO_2 is favoured over CO. This has the consequence that observed C/O ratios in terrestrial atmospheres cannot be relied on to infer the C/O ratio of the protoplanetary disc in which the planet formed.

The initial results of atmospheric modelling for TRAPPIST-1 planets indicate that these planets are likely to have relatively warmer upper atmospheres due to the fact that their host star emits primarily in the infrared, and a portion of this radiation

is then absorbed as it enters the top of the atmosphere. These initial results have not been seen in previous work.

These initial results are the beginning of a database of potential atmospheres on the TRAPPIST-1 planets. It is hoped that these atmospheres can be compared with observations from future observing missions like the James Webb Space Telescope to help constrain the surface conditions of these potentially-habitable planets and ultimately, to help in the search for life.

Acknowledgements

They say it takes a village to raise a child, and the same might be said for the writing of a thesis. I could not have done this without the support network I have in my life, and it is with sincere gratitude that I acknowledge you here.

To my supervisor, Dr. Ralph Pudritz. Your guidance and encouragement throughout this thesis has been invaluable. There were innumerable times when I was stuck and not sure how to proceed, then had a meeting with you and walked out with dozens of new ideas and a renewed belief that I could figure the problem out.

To the other members of my supervisory committee, Dr. James Wadsley and Dr. Nicholas Kevlahan, whose suggestions and questions drove me to make my code better, and Dr. Maikel Rheinstädter who, despite only officially joining my supervisory committee at the last minute, has always taken the time to be supportive of me and the work I've been doing.

To the other members of Ralph's research group. Your expertise, advice and friendship was invaluable.

Ben: we were stuck together pretty much from day one when I was still trying to find my way around the university. If it weren't for you, I might be still wandering around lost. As my fellow astrobiology/Origins Institute student, we spent many of our classes and much of our time together and there's no one I'd rather have gone through that with.

Alex: I've developed a habit of rolling my chair backwards to your desk to ask you questions (sorry for all the times I startled you), and your experience and insight on atmospheres has been so valuable to me. I would particularly like to thank you for so readily processing all of the absorption cross-section data for me.

Matt: my work built off some of your results, and you've always welcomed my questions, but perhaps more importantly, being a year ahead of me, you've been a source of knowledge about what to expect and how to prepare for my own MSc.

Corey: you might be stuck in a group that's heavily planet-dominated, but that didn't stop you from offering me help. Your willingness to help me work through whatever radiative transfer problem I was having trouble with allowed me to make leaps of progress in my code.

To my friends, both in school and out, and to my family. You had faith in me even in the times I'd lost faith in myself.

The other grad students, both in astronomy and astrobiology: you've made this department a wonderful place to be. I can't overstate how much I've loved working with (and distracting) you all.

The mountain biking, dance and climbing communities: sports were how I kept my life balanced (and also how I blew through my physiotherapy health insurance in a matter of months, but I mostly pretend that didn't happen), and these sports and communities brought me such joy through my MSc that I would be remiss to not

acknowledge their value in my life.

Pawel: you came into my life late in this whole endevour, but you jumped in with both feet to be there right when I needed it the most.

My parents: when you're a child, you think your parents know everything and can fix anything. I'm still convinced mine do.

Nathan: you saw it all, the tears and the triumphs, the excitement when something when right and the frustration when it didn't. When I was struggling with a problem, you listened and offered ideas. Even when you were spending long hours of your own at school, with your own research and projects to finish, you stood by me and you held my hand. I love you.

Thank you.

Contents

List of Figures

Chapter 1

Introduction

1.1 Super-Earths and Super-Earth atmospheres

Super-Earths, the most abundant type of exoplanet discovered so far (Howard *et al.*, 2011), are rocky planets with masses ∼1-10 times that of Earth (Seager and Deming, 2010). With diverse atmospheres formed from gas envelope accretion and outgassing (Seager and Deming (2010), Elkins-Tanton and Seager (2008)) and a wide range of atmospheric masses, these planets are of particular interest because of their potential to be Earth-like and thus potentially habitable. Planets less than 1.6 Earth radii, or roughly 3.5 Earth masses, are of particular interest for the search for life because it is thought that planets in this mass range are unable to accrete large gas envelopes, restricting the planet's surface atmospheric pressure to something similar to the terrestrial planets in our solar system (Rogers, 2014).

Of particular interest are Super-Earths orbiting in the habitable zones of M-dwarves, because the orbital period of a planet orbiting an M-dwarf is typically on the order of days, allowing many observations to be performed over a relatively short time period. However, there is some concern about the ability of a planet orbiting an M-dwarf to host an atmosphere due to the planet's proximity to the star and the star's high levels of activity. The study of habitability of planets orbiting M-dwarves is an active field. This is discussed in more detail in Section 1.1.3.

1.1.1 Super-Earth observations

Figure 1.1 shows the distribution of observed exoplanet masses plotted against the planet's orbital period and colour-coded for the temperature of the planet's host star. The data in this figure are from the Exoplanet Orbit Database, a database that collects exoplanet detections from all sources, including Kepler planets and planets discovered through timing, imaging, astronometry and microlensing. A variety of planet types can be seen in this figure, with the cool gas giants, like our own Jupiter and Saturn, located in the upper right of the figure, the Hot Jupiters located in the upper left, and the Super-Earths located in the lower region of the figure. As highlighted in this figure, Super-Earths are the most commonly observed exoplanets: of 5220 planets and planet candidates listed in the Exoplanet Orbit Database (Han *et al.*, 2017), 3637 (69.7%) are less than 10 Earth masses and 1406 (26.9%) are less than 3.5 Earth masses. They are found at all orbital radii, with orbital periods spanning from days to a little over a year. At the time of writing, 52 of the observed Super-Earths orbit within the habitable zone of their host star, making them potentially habitable (Laboratory, 2017), and that number is steadily growing.

Most of these Super-Earths were discovered by the Kepler Space Telescope, which was launched in March 2009 with a goal of finding Earth-like planets around Sun-like stars. Because the Kepler telescope detects planets using transit method, these

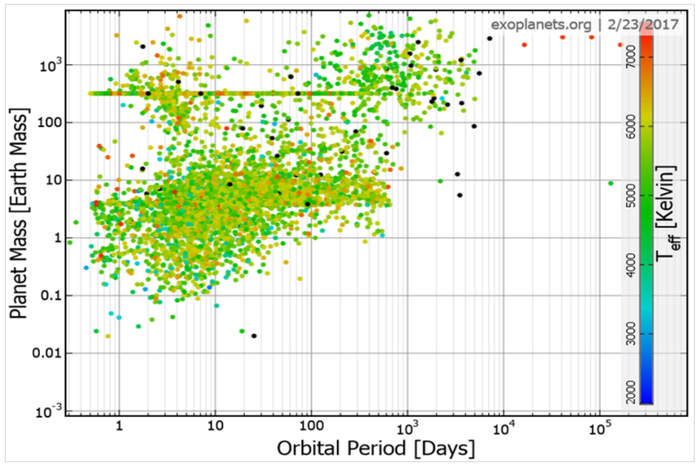

Figure 1.1: Distribution of planet masses showing the prevalence of planets smaller than 10 Earth masses (Super-Earths). Data from the Exoplanet Orbit Database (exoplanets.org).

planet radii were well-constrained but their masses had to be determined using follow-up radial velocity observations. The Kepler Space Telescope operated for five years before its reaction wheels failed, ending the planet-hunting mission that had found 2335 confirmed planets, and 4496 unconfirmed planet candidates that are still waiting for follow-up observations (NASA (2017)). Kepler currently operates the more limited K2 Second Light mission, where it uses its remaining mobility to continue to detect exoplanets, supernovae, star formation, and asteroids and comets, and has, to date, detected 148 confirmed exoplanets, and 520 exoplanet candidates.

Kepler data showed that Super-Earths come in a wide variety of compositions: Figure 1.2 shows the mass-radius distribution of detected planets as compared to spheres of pure hydrogen, water, rock and iron. Super-Earths, falling in the boxed region of this plot, have been observed to have mean densities ranging from pure iron spheres to hydrogen-dominated gassy planets, and this wide range in composition will impact what atmospheres are present on these planets.

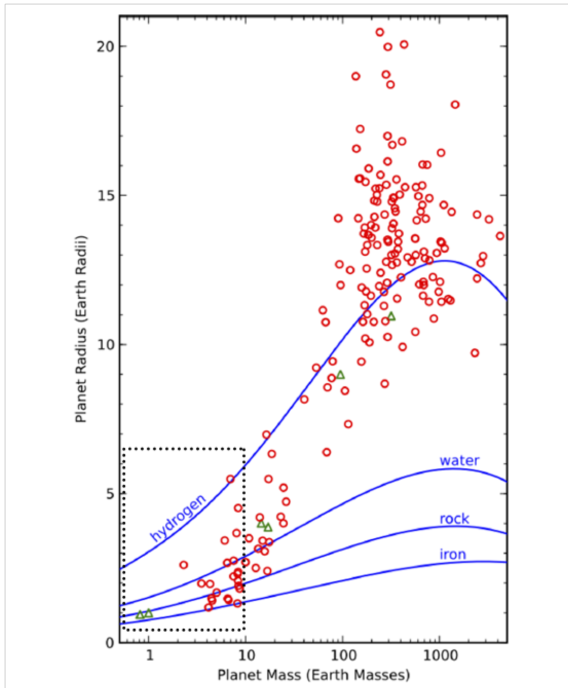

Figure 1.2: The mass-radius distribution of well-characterized planets as compared to spheres of pure hydrogen, water, rock and iron. Red circles are exoplanets and green triangles are planets in our solar system (Figure 2 from Howard *et al.* (2013)). Super-Earths fall into the boxed region of this plot. The planets that lie above the hydrogen line are Hot Jupiters that orbit very close to their host stars, and, as such, are highly inflated from the star's heat

While the Kepler Space Telescope has discovered the large majority of exoplanets, two important discoveries were made in the last year with instruments other than Kepler: Proxima b, detected by the European Southern Observatory (ESO) using radial velocity method, and the TRAPPIST-1 system, discovered using transit photometry with the TRAPPIST telescope.

Proxima b, 1.3 Earth masses, orbits the closest star to our sun, Proxima Centauri, a red dwarf with a mass of 0.123 Msun (Anglada-Escudé *et al.*, 2016). The planet has an equilibrium temperature of 234 K and is thought to be potentially habitable (Anglada-Escudé *et al.* (2016), Barnes *et al.* (2016)) if it can hold onto an atmosphere.

Unfortunately, it appears that the Proxima system is oriented such that the planet will not be visible through transit (Kipping *et al.*, 2017), so detection of an atmosphere on Proxima b will likely have to be by direct imaging. However, Meadows *et al.* (2016), show that James Webb Space Telescope, due to launch in 2018 and discussed in more detail later in this section, could be capable of performing the direct spectrographic observations required to observe an atmosphere around Proxima b, giving studies on this planet an exciting future.

The TRAPPIST-1 system, a system of seven roughly Earth-sized planets orbiting an ultracool M-dwarf (0.082 Msun, 2550 K), was detected through transit photometry Gillon *et al.* (2017), so is also an ideal candidate for follow-up with future missions like James Webb Space Telescope. The light curve from the TRAPPIST-1 system can be seen in Figure 1.3, where transits of each planet are identified. Of particular importance for the search for life, three or four of the seven TRAPPIST-1 planets are thought to lie in the star's habitable zone, with the variation in number of planets in the habitable zone due to two different estimates of habitable zone width and location (Gillon *et al.*, 2017). This system, and its potential habitability, is discussed in detail in Section 3.

Unfortunately, Super-Earths' relatively small size makes it difficult to observe their atmospheres. To date, only three Super-Earth atmospheres have been observed with enough resolution to begin to identify atmospheric constituents: 55 Cancri e, detected in 2011, GJ 1214 b, detected in 2010, and GJ 1132 b, detected in 2017. Of the three, only 55 Cancri e has had follow-up observations to determine more details of the exoplanet's atmosphere: a follow-up study in 2016 (Tsiaras *et al.*, 2016) shows 55 Cancri e's atmosphere is made of hydrogen and helium, with possible

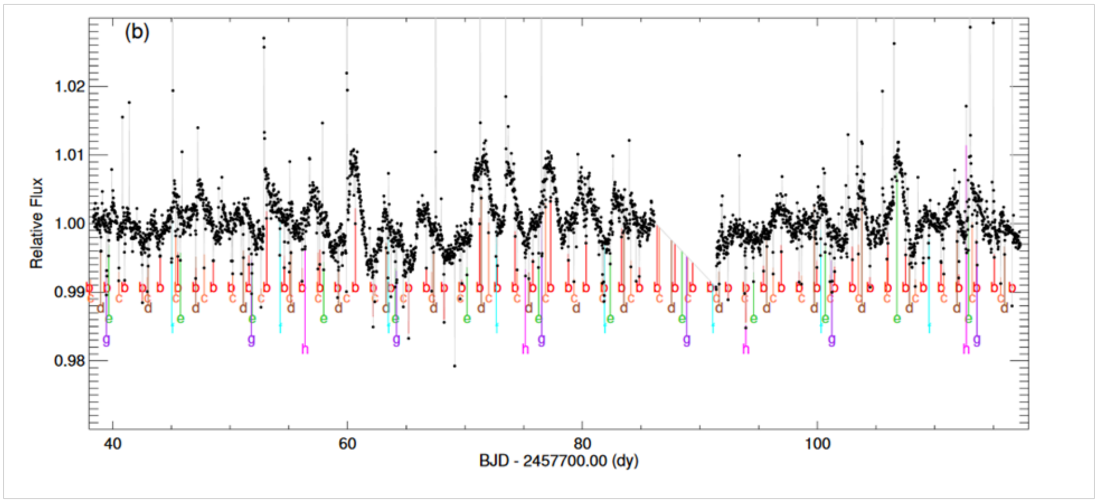

Figure 1.3: TRAPPIST-1 light curve from Kepler K2 showing transits of all planets. The star's rotation appears in the peaks and troughs of the signal (Figure 2b, Luger *et al.* (2017))

hydrogen cyanide. GJ 1214 b and GJ 1132 b, on the other hand, are thought to have atmospheres made of water vapour or thick high-altitude clouds (Berta *et al.*, 2011), and water vapour or methane (Southworth *et al.*, 2016) respectively. The atmospheric detection of GJ 1132 b is shown in Figure 1.4, plotted in comparison with theoretical spectra of hydrogen-dominated atmospheres with varying amounts of water mixed in.

In addition to 55 Cancri e, GJ 1214 b and GJ 1132 b, there have been other, less well-resolved observations of atmospheres on Super-Earths. Of note, two of the planets in the TRAPPIST-1 system mentioned above, planets b and c, had their atmospheres observed in a combined spectrum using Hubble Space Telescpe in 2016 (de Wit *et al.*, 2016). The observation, which revealed a featureless spectrum, was sufficient to rule out cloud-free hydrogen-dominated atmospheres, but was unable to constrain the atmospheric composition further. The featureless spectrum allows for the possibility of water, carbon dioxide, nitrogen or oxygen-dominated atmospheres.

All three of the planets with identified atmospheric consituents are too hot to host

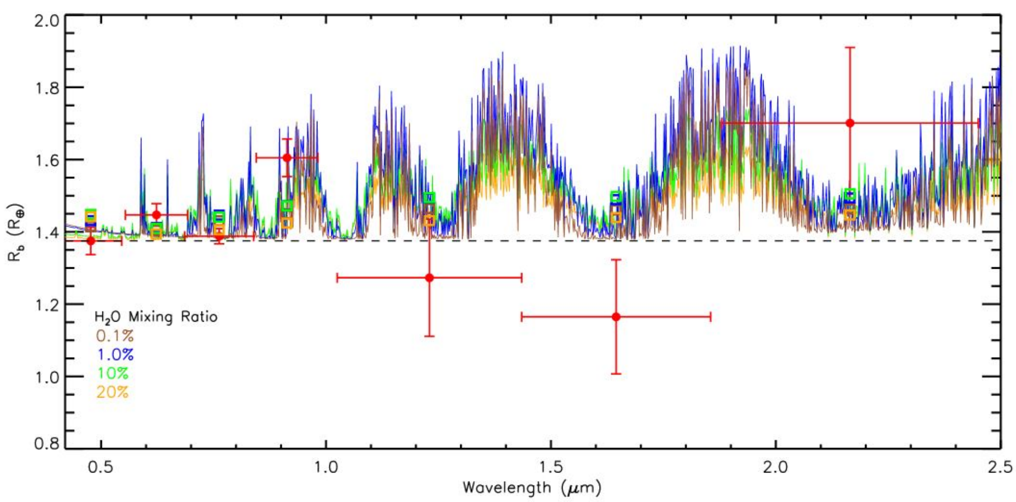

Figure 1.4: Observed and theoretical transmission spectra of GJ 1132 b. Theoretical spectra are for a hydrogen-dominated atmosphere mixed with varying amounts of water by volume. The red points are observations, coloured circles are the band-integrated values of the theoretical spectra and the dashed black line is the baseline radius of the planet (Figure 9, Southworth *et al.* (2016), ©AAS. Reproduced with permission).

life: GJ 1214 b has an equilibrium temperature of 393 K to 555 K (Charbonneau *et al.*, 2009), GJ 1132 b has an equilibrium temperature of 410 K (Southworth *et al.*, 2016), and 55 Cancri e has an equilibrium temperature of more than 2000 K (Tsiaras *et al.*, 2016). While no observations of temperate Super-Earth atmospheres have been performed to date, the number of Super-Earth atmosphere detections will increase in the next few years with the launch of James Webb Space Telescope in late 2018 and follow-up observations of planets identified by the Transiting Exoplanet Survey Satellite, due to launch in early 2018.

The James Webb Space Telescope is a joint NASA, ESA, CSA and Space Telescope Science Institute (STScI) mission that will observe in the near- to mid-infrared (0.6 to 27 micrometers). One of its mission goals is to understand the formation of planets through direct imaging of exoplanets. It will also be capable of transit photometry (Clampin *et al.*, 2007), with unprecedented ability to observe transmission spectra of atmospheres in the infrared. Considered Hubble Space Telescope (HST)'s scientific successor, JWST, with its four highly infrared sensitive cameras, will have up to an order of magnitude more resolution and five times the wavelength coverage (see Figure 1.5 for a comparison of HST and JWST capabilities (Batalha, 2016), ushering in a new era for exoplanet atmospheric characterizations.

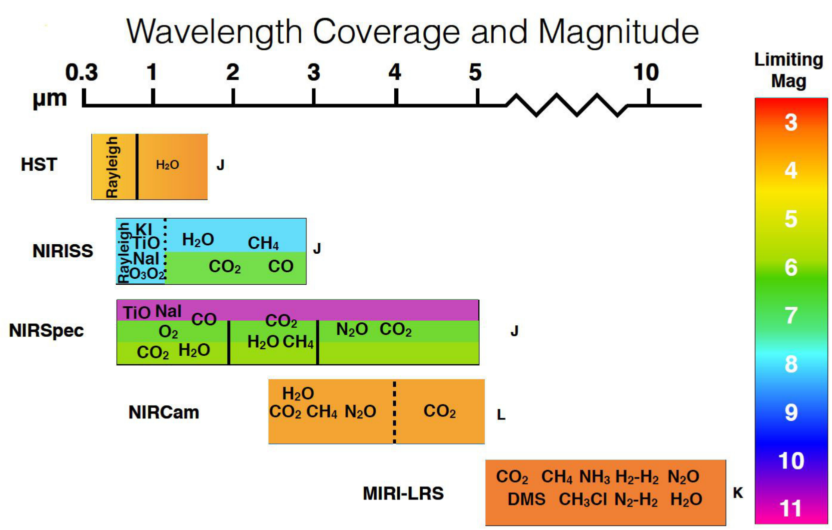

Figure 1.5: A comparison of the capabilities of Hubble Space Telescope (HST) and the four James Webb Space Telescope cameras (NIRISS, NIRSpec, NIRCam and MIRI-LRS). NIRSpec has three levels of resolution of spectroscopy and NIRISS has two. Molecules that can be observed by each camera are identified. Limiting magnitude is the saturating limit of the instrument. J, K and L represent the bands in which the magnitude is defined, where J = 1.25 microns, K = 2.15 microns and L = 3.5 microns.

1.1.2 Atmosphere composition

Atmospheres on planets can be formed in two ways: through accretion of gas from the protoplanetary disc, or through outgassing of volatiles from the planet core itself. This outgassing can occur during planet formation or through later tectonic activity (Elkins-Tanton and Seager, 2008). Gas giants get the large majority of their atmospheres through accretion of gas from the protoplanetary disc, accreting large amounts of hydrogen and helium, and also drawing in the trace gases found in the protoplanetary disc, while small planets whose surface gravity is too weak to retain the hydrogen and helium found in the protoplanetary disc gain the majority of their atmospheres through outgassing. Outgassing can occur either from the planets' slowly cooling cores, which release a steady stream of volatiles through volcanic activity, or through meteorite impacts that release large volumes of volatiles in one impact (Forget and Leconte, 2014). In either of these cases, the volatiles released during outgassing depend on the volatiles available in the solids that make up the planet core.

Super-Earths, being a class of planets that extends from roughly one to ten times the mass of Earth, can be large enough to accrete and retain some hydrogen and helium, along with other trace gases in the disc. However, their relatively large cores also mean that outgassed volatiles could have a large impact on atmospheric composition. Smaller Super-Earths likely have a thinner, outgassed atmosphere, while larger Super-Earths can have larger atmospheres dominated by hydrogen and helium, making Super-Earths a class of planet with a wide diversity of atmosphere composition and mass. Because hydrogen and helium do not absorb much incoming stellar radiation (infrared to visual) or outgoing infrared radiation from the planet core, it becomes important to identify and model the other gases in the atmosphere that do the majority of the absorption of radiation. Because the other gases found in an atmosphere are either trace gases from the protoplanetary disc or volatiles from outgassing, planet formation history becomes important.

Since composition of the protoplanetary disc changes radially, with different species condensing into solids at different points in the disc, location of planet formation, and subsequent track of planet migration dictate which solids are accreted into the planet core and which volatiles are accreted in an atmosphere. If a planet forms far out in the protoplanetary disc, it can accrete solids made of a variety of ices (water, carbon monoxide, carbon dioxide etc), and, if it migrates inwards later, it can then outgas some of these solids to form an atmosphere. On the other hand, a planet forming in the hot inner region of the protoplanetary disc will not have access to ices, and will be left to form from the rocky and metal-rich solids available in the inner disc. Likewise, if a planet accretes an atmosphere by drawing gas from the protoplanetary disc, a planet accreting far out in the disc is able to accrete different gases than a planet accreting an atmosphere close to the star.

Cridland *et al.* (2016) and Cridland *et al.* (2017) have modeled the trace species found in primordial atmospheres on Super-Earths and gas giants. They use the concept of planet traps, inhomogeneities in the protoplanetary disc where planets slow their migration and accrete large amounts of solids and gas. They identify three trapping regions: heat transition, dead zone and water ice line, which were first identified by Hasegawa and Pudritz (2011). The heat transition trap occurs at the radius where the protoplanetary disc transitions from being heated primarily through viscous heating to being heated through direct irradiation: the inner disc, where viscous heating occurs, has a high surface density, while the outer disc's surface density is lower. The dead zone trap occurs where the disc becomes less turbulent, which allows dust to settle more quickly than in the active turbulent disc just beyond the trap. This creates a dust wall that back-scatters radiation and creates a temperature inversion that causes a thermal barrier to migration. The ice line trap occurs at the radius at which water sublimates from ice to vapour. The opacity of the disc thus changes, changing the local surface density and temperature. All of these traps can migrate through the disc as the disc ages and cools, as shown in Figure 1.6.

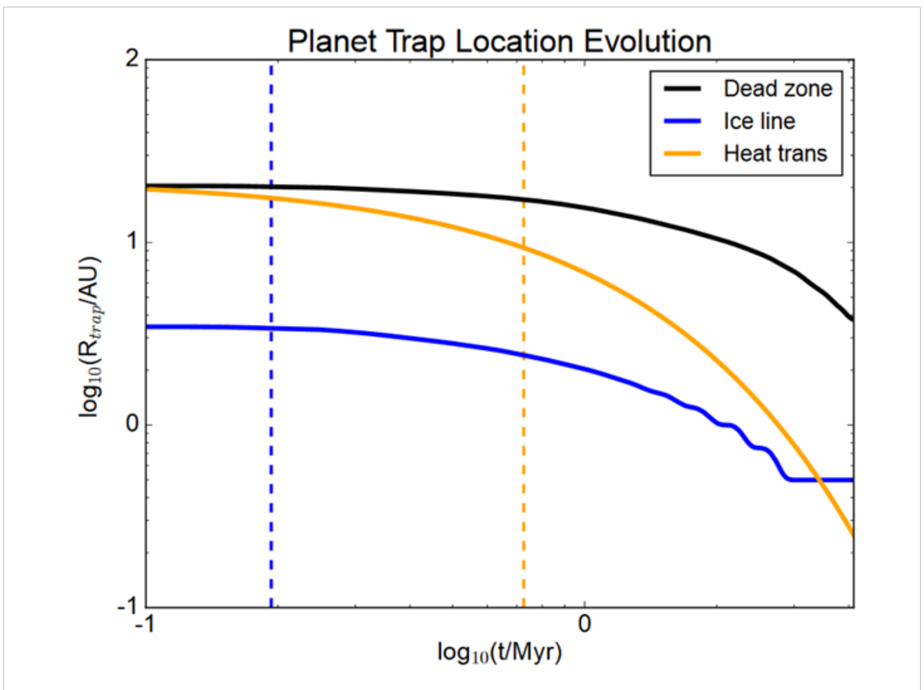

Figure 1.6: Evolution of planet trap locations as the disc ages. The vertical dotted lines indicate location and time where the planet's radial evolution uncouples from the planet trap's radial evolution (Figure 10, Cridland *et al.* (2016))

Because the planet traps are located at different radii in the disc, a planet formed in the heat transition trap will have access to different solids and gases than a planet formed in the dead zone or ice line traps. Cridland *et al.* (2016) identify atmospheres characteristic of each trap, and show the variety of trace gases accreted. This is outlined in Table 1.1.

Table 1.1: Minor gas abundance as a percentage of mass not in H_2 and He (Table 5, Cridland *et al.* (2016))

	Dead zone %	Ice line %	Heat transition %
H_2O	99.84	67.92	61.15
CO	< 0.01	30.40	36.70
H	< 0.01	0.02	0.1
CO_2	< 0.01	0.32	0.09
N_2	< 0.01	< 0.01	1.85
NH_3	< 0.01	0.69	< 0.01
HCN	0.12	0.2	< 0.01
CH_4	< 0.01	0.45	0.11
HNC	0.02	< 0.01	< 0.01

Since atmospheres can also be formed or changed through outgassing of volatiles from solids, it is important to identify the solids that make up a Super-Earth planet core. Alessi *et al.* (2017) model the chemical composition of Super-Earths, identifying the makeup of these planets based on their formation history. Like Cridland *et al.* (2016), Alessi *et al.* (2017) identify planet traps as locations of planet formation, and use heat transition, ice line and dead zone traps to form planets. However, instead of using x-ray radiation to create the dead zone like Cridland *et al.* (2016), Alessi *et al.* (2017) uses cosmic rays. This changes the location of the dead zone in the disc, with Cridland *et al.* (2016)'s X-ray dead zone being further out in the ice-rich reaches of the disc, and Alessi *et al.* (2017)'s cosmic ray dead zone located closer to the host star, in the dry region inside the ice line.

Alessi *et al.* (2017) form planets with a wide variety of compositions: their Super-Earths range from dry and rocky planets to planets with substantial water, with planets formed at the ice line having large amounts of water, and planets formed in the dead zone having very little water. Figure 1.7 (Figure 12, Alessi *et al.* (2017)) shows the range of compositions possible for Super-Earths based on formation history. In this figure, elements found in the core include iron and nickel compounds ($FeAl_2O_4, Fe_3O_4, FeS, Ni_3S_2, FeO$), while elements found in the mantle are rocky, containing magnesium and silicon ($CaMgSi_2O_6, MgSiO_3, Mg_2SiO_4, NaSiO_3$). In this model, ice is made simply of water ice.

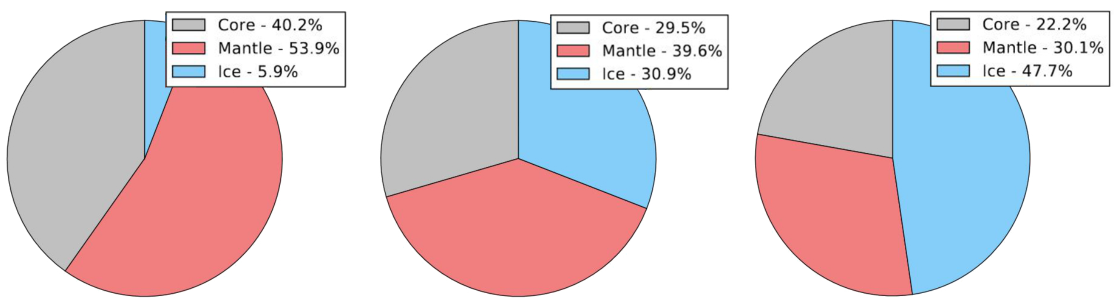

Figure 1.7: Variation in solid mass abundances for Super-Earths: the dead zone planet (left) that forms inside the ice is very dry, and the ice line (middle) and heat transition (right) planets have more ice because they form in the far out, icy regions of the disc (Figure 12, Alessi *et al.* (2017))

Not all of the solids that make up a Super-Earth's core will be outgassed to form an atmosphere. Elkins-Tanton and Seager (2008) model the volatiles outgassed during planet formation from planets with a variety of compositions. They use the extreme ends of planet bulk composition: mostly dry planets that are formed by rocky, iron-bearing planetesimals, and planets that are formed in the outer solar system, becoming rich in ices and volatiles. These extremes line up neatly with the planets formed by Alessi *et al.* (2017), making it possible to estimate the outgassed atmospheres that would appear on this group's planets. Elkins-Tanton and Seager (2008) use four models: a planet made of undifferentiated primitive (chondritic) material with no added water, a planet made of primitive material with added water, a differentiated (achondritic) planet with no added water, and a differentiated planet with added water. They found that these planets outgas hydrogen, water and carbon compounds, with some carbon compounds including oxygen.

General results indicate that an undifferentiated planet forms an atmosphere by reacting metallic iron with water, forming hydrogen and iron oxide. If the iron is depleted before water is (i.e. in a planet with water added, or a planet with very little iron), the atmosphere is dominated by water and carbon compounds, with trace amounts of hydrogen. If the water is depleted before the iron, the atmosphere is dominated by hydrogen and carbon compounds, with traces of helium and nitrogen. A differentiated planet, on the other hand, forms an atmosphere through the cooling and outgassing of the silicate mantle, yielding an atmosphere of water and carbon compounds, with traces of helium and nitrogen.

Like Elkins-Tanton and Seager (2008), Schaefer and Fegley Jr. (2009) also modeled outgassed atmospheres, studying atmospheres formed during outgassing from accretion impacts, and using a larger variety of chondritic materials in their planetesimals model. Their results confirm those found by Elkins-Tanton and Seager (2008): Schaefer and Fegley Jr. (2009) also form atmospheres dominated by water, carbon dioxide, hydrogen or carbon monoxide, with a variety of trace species. The dominant species depends on what chondritic material is used to form the planet core.

Outgassed and accreted atmospheres can evolve post-formation: atmospheres can be lost due to thermal escape or non-thermal methods such as interactions with stellar wind that strip away an atmosphere or impacts of asteroids or comets that eject hot plumes of atmosphere into space. Smaller planets are more likely to experience atmosphere loss (both thermal and non-thermal) due to their lower gravity, and thermal escape affects lighter atoms and molecules like hydrogen and helium over heavier molecules like carbon dioxide because, for a given atmospheric temperature, lighter molecules can reach higher velocities, to the point that they can overcome a planet's gravity and reach escape velocity (Forget and Leconte, 2014).

Of particular concern for potential habitability, water can be lost through photodissociation, which can separate the water molecules into hydrogen and oxygen. Hydrogen molecules in the atmospheres of smaller Super-Earths can then escape to space due to their small size, which allows them to gain significant velocity when heated by the planet's host star. If a planet has no liquid water ocean, either from being too hot for water in the atmosphere to condense, or from being formed with limited water, no water cycle can be established, so atmospheric water cannot be replenished or sustained. This leaves planets with dry atmospheres often dominated by carbon dioxide, like the atmospheres found on Venus and Mars (Elkins-Tanton and Seager, 2008).

All of these factors impacting atmospheric formation and evolution mean that Super-Earths can be expected to have a wide variety atmospheric compositions, and work must be done to determine which of these compositions is likely to yield Earth-like, or potentially-habitable, surface compositions.

1.1.3 Habitability of Super-Earths

Habitability is classically defined as the ability of a planet to host liquid water on its surface (Kasting *et al.*, 1993). For a planet to have liquid water, it must have a surface, must orbit in a temperate region around its host star, and must have an atmosphere thick enough so that water does not boil away from the lack of pressure, but not so thick that the surface becomes too hot and the water boils away due to heat. Mars and Venus are examples of these two atmospheric extremes: Mars's atmosphere is too thin to allow lasting liquid water on the surface, and any water that was once on Venus has boiled away into the atmosphere where it was stripped of its hydrogen due to photodissociation, and the hydrogen was lost due to thermal escape. Since Super-Earths are all thought to have a rocky core, satisfying the requirement for a habitable planet to have a surface, the focus of habitability studies is typically the planet atmosphere and temperature.

Habitability of planets orbiting M-dwarves is of particular interest because M-dwarves are the most common star type, and planets in the habitable zone of an M-dwarf have orbital periods of only days, allowing for many observations of a single planet to be made in a relatively short period of time. There has been significant debate about the conditions on M-dwarf planets, due in large part to the high level of activity of these types of stars: M-dwarves, particularly in their early life, are very active, throwing out high levels of far UV and X-ray photons that have the potential to strip an atmosphere from a nearby planet.

Wheatley *et al.* (2017) found that planets in the TRAPPIST-1 system could lose their entire atmosphere over 3 billion years due to x-ray and UV radiation, and Garraffo *et al.* (2016) found that the Proxima b could experience stellar wind pressures more than two thousand times that experienced on Earth, which could strip an atmosphere off the planet. However, Wheatley *et al.* (2017) acknowledged their model was simplistic and an upper limit to mass loss, and, because M-dwarves are most active in their youth, planets that formed further out in the protoplanetary disc, and thus further from the active young star, then migrated inward when the star was older could potentially retain an atmosphere.

An atmosphere could also be retained in the presence of a magnetic field: magnetic fields can protect an atmosphere from being stripped away, and Barnes *et al.* (2016) indicate that Proxima b could have a magnetic field sufficient to protect its atmosphere from stellar winds. Regardless of which mechanism allows an atmosphere to be retained, perhaps most promisingly, two of the only three Super-Earth atmospheric observations, GJ 1132 b (Southworth *et al.*, 2016) and GJ 1214 b (Charbonneau *et al.*, 2009) (see Section 1.1.1), belong to planets orbiting M-dwarves. GJ 1132 b, 1.6 Earth masses, orbits with a period of 1.6 days, which is inside the inner limit of the habitable zone, meaning it is subject to higher levels of irradiation from the star, and thus is more likely to experience higher levels of atmospheric escape, than a planet in the habitable zone. The observed atmosphere is thick, and likely made of methane or water (Southworth *et al.*, 2016). GJ 1214 b, 6.55 Earth masses, also orbits inside the inner limit of the habitable zone of its star with a period of 1.58 days (Charbonneau *et al.*, 2009). Its thick atmosphere is likely predominantly water (Berta *et al.*, 2011).

However, it should be noted that the presence of an atmosphere does not necessarily mean hospitable surface conditions: as noted by O'Malley-James and Kaltenegger (2017), even in the presence of an atmosphere, UV surface irradiation could be deadly to even the most extremophile life that we know of. O'Malley-James and

Kaltenegger (2017) indicate that the presence of oxygen in the atmosphere, which would photodissociate in the presence of ultraviolet radiation to form ozone in a layer much like Earth's own, could be sufficient to protect the surface of a planet. It is also possible that hazes, formed through photochemical reactions between incoming UV radiation and molecules in the atmosphere, could protect a planet's surface from UV radiation, making an otherwise highly-irradiated planet potentially habitable (Arney *et al.*, 2017).

Given the importance of atmospheres in determining habitability of a planet, detection of more atmospheres on Super-Earths orbiting M-dwarves is potentially the single most important indicator for potential life on these sorts of planets. By modeling a range of potential atmospheres on Super-Earths and determining which ones yield temperate surface conditions, this work strives to provide guidelines that can be used to help determine which observed atmospheres are potentially habitable.

1.2 Atmospheric Modelling

Atmospheric modelling is primarily used to determine temperature and pressure structures of an atmosphere and to predict transit spectra on of a planet. It can give insight into conditions on a planet that cannot otherwise be observed, and is an important tool in understanding exoplanets, both observed and theoretical.

1.2.1 Previous work

Numerous groups have modelled planetary atmospheres, starting with Earth's atmosphere, moving to atmospheres in our solar system and finally to exoplanetary atmospheres as observations reach farther and farther into space.

The principles used to model Earth's atmosphere in the 1970s are still valid in exoplanet atmosphere models today. Ramanthan and Coakley Jr. (1978) were one of the first groups to build a radiative-convective model for Earth's atmosphere. They modelled the atmosphere as one-dimensional, considering only temperature and pressure variation with altitude, and used a two stream radiative model, which approximates radiation as travelling in only two directions: incoming radiation from the star and outgoing radiation from the planet's surface. They simplified the model further by assuming all incoming radiation was in the visual waveband and all outgoing radiation was in the infrared band and ran their model until it reached radiative equilibrium, which occurs when net flux at every point in the atmosphere goes to zero. They applied a convective adjustment to their radiative model, which limited the temperature gradient of the atmosphere: if the temperature gradient is too steep, convection occurs, and the change in temperature with altitude follows the convective lapse rate, or the maximum lapse rate allowed in an atmosphere. This is described in more detail in Section 2.1.3 and Section 3.2.2.

When Kasting *et al.* (1993) modelled widths of habitable zones around main-sequence stars, they used a one-dimensional radiative-convective model for Earth-like planets similar to that used by Ramanthan and Coakley Jr. (1978). However, in considering only Earth-like planets around sun-like stars, this group neglected influence of stellar type and planet type on habitable zones and habitability.

Current models on potentially-habitable planets attempt to account for the wide range of Super-Earth atmospheres expected, and many groups focus on predicting the spectrum observed from a planet. For example, Kempton (2010) modelled observable spectra of a thin water atmosphere in comparison to a thick hydrogen atmosphere, while Miller-Ricci (2008) used a model to determine that it is possible to tell if a planet's atmosphere is hydrogen rich or hydrogen poor through transmission spectra.

Other groups focus on modelling the atmosphere of a specific planet: von Paris *et al.* (2011) used atmospheric models to study habitability in the Gliese 581 system, calculating temperature and pressure profiles for a potentially-habitable Super-Earth based on an atmosphere composition assumed to be Earth-like with varying levels of carbon dioxide, and O'Malley-James and Kaltenegger (2017) used a one-dimensional radiative-convective code to determine UV surface habitability of the TRAPPIST-1 system, assuming Earth-like or early Earth-like atmospheric compositions.

While there has been a focus in the last few years on modelling potentially-habitable planets, either modelling their surface conditions or modelling how they can be detected, to date, no group has modelled atmospheres of potentially-habitable exoplanets while considering the planet's formation history. Because planet formation history directly impacts the planet's atmospheric composition and atmospheric composition can dramatically change a planet's surface conditions (see Section 1.1.2), it is important to consider probable atmospheric compositions rather than to simply assume an Earth-like atmosphere exists.

1.2.2 Goals of this thesis

This thesis aims to model atmospheres of potentially-habitable exoplanets using atmospheric compositions based on the planets' likely formation history. The model used, described in Section 3.2, calculates the atmosphere's temperature and pressure structure. This can ultimately be used to create a catalogue of atmospheres that are likely to be observed and identify which atmospheres yield Earth-like surface conditions. The hope is that future atmospheric observations can be cross-referenced with the catalogue of atmospheres presented in this thesis, and, if an observed atmosphere has the same characteristics as one of the modelled potentially-habitable atmospheres, the observed atmosphere can be identified as a target for follow-up observations and more extensive modelling.

Chapter 2

Atmospheric physics and modelling principles

2.1 Atmospheric science

Atmospheric science is a field that combines a range of principles from both physics and chemistry, and an understanding of it is necessary to develop atmospheric models. Key subjects in atmospheric science are highlighted below.

2.1.1 Conservation of mass and hydrostatic equilibrium

At equilibrium, an atmosphere is in hydrostatic equlibrium. The equation for hydrostatic equilibrium can be derived by simplifying the three-dimensional Navier-Stokes equation.

The Navier-Stokes equation for conservation of momentum governs the motion of fluids and is given by Equation 2.1, where ρ is the atmospheric density, $\boldsymbol{u}$ is the velocity, and $\boldsymbol{f}$ is the force density, which is made up of whatever forces are acting on the fluid (e.g. gravity, pressure, Coriolis, friction).

$$\frac{\partial}{\partial t}(\rho \boldsymbol{u}) + \nabla \cdot (\rho \cdot \boldsymbol{u}\boldsymbol{u}) = \boldsymbol{f} \tag{2.1}$$

The Navier-Stokes equation is solved in tandem with the continuity equation (Equation 2.2), which represents the conservation of mass.

$$\frac{\partial \rho}{\partial t} + \nabla \cdot (\rho \boldsymbol{u}) = 0 \tag{2.2}$$

In an atmosphere in hydrostatic equilibrium, the Navier-Stokes equation can be simplified by assuming that velocity is zero and pressure is uniform in the x and y directions, or $u = v = \frac{\partial p}{\partial x} = \frac{\partial p}{\partial y} = 0$, which leaves only the terms in the z direction, shown in Equation 2.3. Additionally, since the atmosphere is in steady state, the time-dependent partial differential $\frac{\partial}{\partial t}$, goes to zero. This is the hydrostatic equilibrium equation, which is used to determine the pressure and density structure of the atmosphere.

$$\frac{\partial p}{\partial z} + \rho g = 0 \tag{2.3}$$

2.1.2 Radiative transfer

Energy in an atmosphere is primarily transported though radiation. Specific intensity, shown in Equation 2.4 describes energy, E, being radiated at an angle $cos\theta$ into a solid angle $d\Omega$, per frequency $d\nu$, unit surface area dA and time dt.

$$I(\nu) = \frac{dE(\nu)}{dA\, cos\theta\, dt\, d\nu\, d\Omega} \tag{2.4}$$

Radiative transfer, or the transfer of radiative energy through an atmosphere, can be described using Equation 2.5, where $B(\nu, T)$ is the radiation emitted by the atmosphere at temperature T.

$$\frac{dI(\nu)}{d\tau(\nu)} = -I(\nu) + B(\nu, T) \tag{2.5}$$

Assuming no scattering (see Section 2.2.2 for a discussion on the choice to neglect scattering), specific intensity I_ν can be expressed in terms of radiation coming from the source (the star or the surface of the planet) and radiation emitted by the atmosphere by integrating Equation 2.5. Equation 2.6 shows specific intensity at any point in the atmosphere, where $I(\nu, 0)$ is the incoming radiation from the source, $\pi B(\nu, T(\tau_\nu^{'}))$ is the radiation that is emitted by the atmosphere and the location in the atmosphere is given by optical depth τ_ν which is a proxy for altitude (Pierrehumbert, 2010).

$$I(\nu, \tau_\nu) = I(\nu, 0)e^{-\tau_\nu} + \int_0^{\tau_\nu} \pi B(\nu, T(\tau_\nu^{'}))e^{-(\tau_\nu - \tau_\nu^{'})} d\tau_\nu^{'} \tag{2.6}$$

Optical depth is a measure of how much radiation is absorbed in a gas relative to how much is transmitted. An atmosphere with a high optical depth absorbs a large amount of radiation and is thus raised to a higher temperature than an atmosphere with a low optical depth. Frequency-dependent optical depth can be calculated using Equation 2.7 (Pierrehumbert, 2010), where κ_ν is the frequency-dependent opacity of the atmosphere, g is the gravitational acceleration of the planet, P_0 is the planet's surface pressure and $P(z)$ is the pressure at the altitude of interest. This equation arises directly from hydrostatic balance, shown in Equation 2.3, and the definition of optical depth: $\tau_\nu = \int_0^z \frac{\kappa_\nu \rho}{cos\theta} dz$ (Carroll and Ostlie, 2007).

$$\tau_\nu(z) = \frac{-2}{g} \int_{P_0}^{P(z)} \kappa_\nu(z) dP \tag{2.7}$$

Optical depth is frequency dependent because the opacity of an atmosphere is frequency dependent (see Figure 2.1). This arises because the atomic and molecular transitions of chemical species in the atmosphere absorb radiation at a wide variety of frequencies.

There is a variety of ways of calculating mean opacity, or opacity averaged over all frequencies, but the Rosseland mean opacity, calculated using Equation 2.8 (Carroll and Ostlie, 2007), is most commonly used for atmospheres.

$$\frac{1}{\bar{\kappa}} = \frac{\int_0^\infty \frac{1}{\kappa_\nu} \frac{\partial B_\nu(T)}{\partial T} d\nu}{\int_0^\infty \frac{\partial B_\nu(T)}{\partial T} d\nu} \tag{2.8}$$

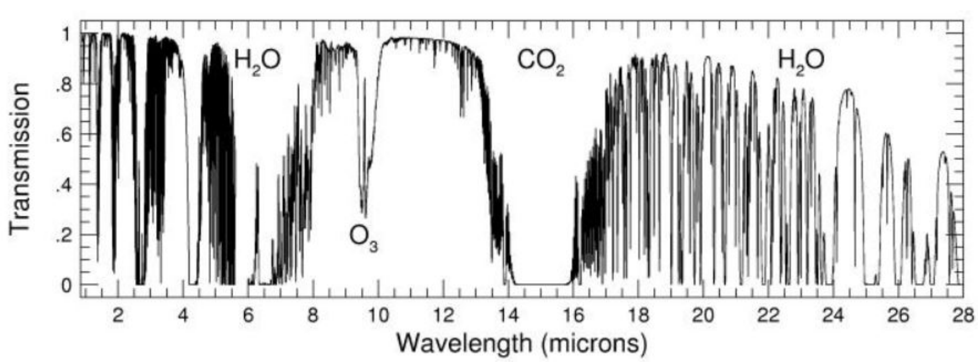

Figure 2.1: Transmission of infrared radiation through Earth's atmosphere as a function of wavelength. Transmission is inversely proportional to opacity so this figure shows how dependent opacity is on wavelength or frequency, highlighting the need for proper handling of opacity

With opacities and optical depths calculated, specific intensity can be integrated over angle to find specific radiative flux (Equation 2.9 (Carroll and Ostlie, 2007)), or the net energy passing through a unit area per second per frequency. Here, we let $cos\theta = \mu$ and $sin\theta = d\mu$.

$$F(\nu, \tau_\nu) = \int_\Omega I(\nu, \tau_\nu) cos\theta d\Omega = \int_0^{2\pi} \int_{-1}^{1} I(\nu, \tau_\nu) \mu d\mu d\phi \tag{2.9}$$

In cases where there is no dependence on angle ϕ, Equation 2.9 simply becomes Equation 2.10.

$$F(\nu, \tau_\nu) = 2\pi \int_{-1}^{1} I(\nu, \tau_\nu) \mu d\mu \tag{2.10}$$

Angle μ is the angle at which the radiation is entering or leaving the atmosphere. In a two-stream approximation, it is assumed that all radiation is entering the atmosphere at a fixed angle and all radiation is leaving the atmosphere at a fixed angle. This angle represents the average angle of incoming and outgoing radiation and varies from simulation to simulation but typically ranges from $\mu = 1/2$ to $\mu = 2/3$, which assumes that the radiation field remains approximately isotropic (Pierrehumbert, 2010). For the purposes of this thesis, $\mu = 1/2$ is selected as per Pierrehumbert (2010). This selection of μ is what causes the constant of 2 to appear in Equation 2.7.

Frequency-dependent flux $F(\nu, \tau_\nu)$ can be integrated to find net flux, shown in Equation 2.11. Note the switch from using optical depth τ_ν to altitude z for the location in the atmosphere. This is done for simplicity: optical depth changes as a function of frequency (for example, carbon dioxide has a high optical depth in infrared bands but a low optical depth in visible bands) but is calculated as a function of altitude for all frequencies (see Equation 2.7 where the dependence on altitude z is explicit). A two-stream approximation would yield two equations for flux, one for flux travelling downwards in the atmosphere, and one for flux travelling upwards.

$$F(z) = \int_{\nu} F(\nu, \tau_{\nu}) d\nu \tag{2.11}$$

When an atmosphere reaches equilibrium, the net flux at every point in the atmosphere goes to a constant value, as shown in Equation 2.12, where $F_{-}(z)$ is the downgoing flux and $F_{+}(z)$ is the upgoing flux (Ramanthan and Coakley Jr., 1978). This constant is zero if the atmosphere is only heated through radiative means, but can be non-zero if other sources of heat, such as tidal heating or radioactive decay, are present.

$$F_{-}(z) + F_{+}(z) = C \tag{2.12}$$

Solving radiative transfer within the atmosphere determines the lapse rate, or temperature change as a function of altitude of the atmosphere, which allows temperature at any point in the atmosphere to be determined. Additionally, in the thin atmospheres on rocky planets, incoming radiation from the star has the effect of heating the surface of the planet more than it heats the atmosphere: the planet's surface absorbs all frequencies while the atmosphere typically absorbs dominantly in the infrared. This temperature discontinuity caused by radiation and radiative transfer is what drives convection, described below, in the lower regions of the atmosphere (Seager, 2010).

2.1.3 Convective adjustment

An atmosphere becomes unstable and convection occurs if the temperature change as a function of altitude is larger than a certain value. This value, given by the Schwarzschild criterion, and shown in Equation 2.13, is used to determine the stability of a gas against convection for everything from planet atmospheres to stars. It is a function of both the planet's gravitational acceleration g and the amount of energy that can be added to an atmosphere before it increases in temperature, expressed through the atmosphere's specific heat at constant pressure c_p. As long as the Schwarzchild criterion is true, the atmosphere is stable against convection. If the temperature gradient in the atmosphere is so large that the Schwarzchild criterion is violated, convection occurs (Ramanthan and Coakley Jr., 1978).

$$\frac{-dT}{dz} < \frac{g}{c_p} \tag{2.13}$$

When convection occurs, the temperature change as a function of altitude can be approximated to simply follow the convective, or adiabatic, lapse rate of the atmosphere. The adiabatic lapse rate is typically taken to be $\frac{dT}{dz} = \frac{-g}{c_p}$, or the dry convective lapse rate. However, if the atmosphere is saturated by water or another condensing species, air follows the moist convective lapse rate, which is shallower than shallower than the dry convective lapse rate. Because clouds and the effects of condensing species are not considered in this model, convection is modelled using the dry lapse rate only.

Convection typically occurs in the lower regions of a planet's atmosphere because the atmosphere becomes unstable due to the large change in temperature with altitude in the lower atmosphere and planet's relatively hot surface, both of which cause vertical motion in the atmosphere. This drives such a region out of radiative equilibrium. However, the atmosphere remains in radiative-convective equilibrium, with the equilibrium condition being described by Equation 2.14 where $F_c(z)$ is the flux from convection. It can be seen that, if the convective flux term goes to zero, the system returns to pure radiative equilibrium shown in Equation 2.12 (Ramanthan and Coakley Jr., 1978).

$$F_{-}(z) + F_{+}(z) + F_c(z) = 0 \tag{2.14}$$

2.1.4 Atmospheric chemistry

Atmospheric chemistry has a large impact on the amount of radiation that is absorbed by an atmosphere. Because radiation from planets peaks in the infrared, gases that absorb in the infrared act as greenhouse gases, absorbing large amounts of the upgoing radiation from the planet's surface and causing the planet to warm. Thus, the composition of the atmosphere is important to know, since even seemingly small amounts of a greenhouse gas can have significant impact on the atmosphere's temperature: Earth's atmosphere, for example, contains only 0.04% carbon dioxide and 0 to 4% water vapour, depending on the location and local weather, but these greenhouse gases have the effect of raising the planet's surface temperature more than 30 K, from the planet's equilibrium temperature of 255 K to its average surface temperature of 288 K.

The simplest way to handle atmospheric chemistry is to assume the atmosphere is in chemical equilibrium, and this is customary in the modelling of exoplanet atmospheres (Beuther *et al.*, 2014). This assumption is a good starting place; however, a number of things can drive an atmosphere away from equilibrium. Most importantly, photochemistry, or chemistry initiated by absorption of a high energy photon, can destroy molecules that would otherwise appear and can drive the creation of molecules like the ozone that appears in Earth's atmosphere (O'Malley-James and Kaltenegger, 2017), or photochemical hazes like those in Titan's atmosphere (Arney *et al.*, 2017). In Earth's atmosphere, photochemistry occurs in the upper regions so does not impact the planet's surface temperature substantially. The same may not be true for exoplanetary atmospheres: hazes, produced through the interaction of UV radiation and methane in the atmosphere, can substantially increase the atmosphere's opacity and reduce the amount of radiation that reaches the planet's surface (Arney *et al.*, 2017).

Nonetheless, assuming the planet atmosphere is in chemical equilibrium is still a valid starting place particularly when the activity of the planet of interest's host star is unknown since stellar activity drives photochemistry, and any model that uses chemical equilibrium can yield valuable insights to the potential temperature-pressure structure of the atmosphere.

2.2 Atmospheric modelling

Atmospheric modelling is often done to determine the temperature-pressure, or thermal, structure of the atmosphere, and can also be used to determine cloud locations, local weather patterns or heat flow from the hot side of a tidally-locked planet to the cold side. Modelling an atmosphere typically starts with the thermal structure of the atmosphere (Ramanthan and Coakley Jr., 1978), with other model parameters being determined once the thermal structure of the atmosphere has been solved.

2.2.1 1D and 3D models

Atmospheric models come in two general classes: one-dimensional and three-dimensional models. Three-dimensional models, or global circulation models (GCMs) model the cirulation of a planet's atmosphere, as the name implies. Because they model the flow of the atmosphere around the planet, they can provide information on the local changes in atmospheric temperature, pressure, cloud cover, atmospheric chemistry and wind conditions and are thus important for determining temperature varience as a function of latitude, location of jet streams and heat transfer between hot and cold locations on a planet. In exoplanet modelling, they can be vital in determining if a tidally-locked planet is able to redistribute heat from the hot side of the planet to the cold side, which could be important for the emergence of life on these such planets.

However, three-dimensional models are computationally expensive and require a large amount of information about the planet in question. Many of the inputs required by a three-dimensional model cannot be measured for exoplanets at this point: the planet's rotation rate, inclination, topography and local albedo among others all impact the three-dimensional model but are unknown for the large majority of exoplanets and assumptions must thus be made for these parameters.

One-dimensional models, on the other hand, are much simpler than three-dimensional models. They are relatively computationally inexpensive, but can be used to determine the average temperature-pressure structure of an exoplanet's atmosphere without requiring the same number of assumptions that a three-dimensional model does. They can also be used in tandem with an emission spectra model to determine the planet's likely emission or transmission spectrum, which is useful for future observations (see Section 1.2.1 for examples of one-dimensional models). The speed of a one-dimensional model allows for numerous runs to be performed for a single planet, allowing researchers to create a range of likely of atmospheres for a single planet. Because of their speed and usefulness in determining average atmospheric conditions and potential observable spectra, one-dimensional models are the standard for exoplanet atmospheres at this point.

2.2.2 Scattering and absorption

Radiation interacts with an atmosphere through scattering or absorption. Scattering complicates radiative transfer, so many models assume atmospheres absorb only (Miller-Ricci, 2008).

When scattering occurs, radiation that was travelling in one direction is redirected and begins travelling in another direction, which has the effect of coupling radiation streams, making relatively simple models like the two-stream approximation described in Section 2.1.2 impossible to employ. When scattering occurs, no analytical solution of the radiative transfer equation is possible, so scattering must always be approximated and solved numerically. This can be done in a variety of ways. For example, Jimenez-Aquino and Varela (2005) approximates scattering using an estimated internal source function, Ramanthan and Coakley Jr. (1978) assumes each photon only scatters once and approximates that scattering using a diffusivity factor, and Miller-Ricci (2008) treat scattering by simply increasing surface albedo.

Because clouds are the dominent source of scattered radiation in an atmosphere, models that neglect scattering imply the assumption of a cloud-free atmosphere (Kasting *et al.*, 1984). Because the cloudiness of Super-Earth atmospheres is not constrained at this point, and because of the complicated nature of scattering, scattering is neglected for this model.

Of note, because scattering primarily occurs at higher frequencies and is not significant in the infrared Miller-Ricci (2008), absorption-only models will perform better for planets orbiting cool stars whose emission is primarily in the infrared than they will for planets orbiting Sun-like stars that produce significant radiation in high frequencies.

2.2.3 Description of model

The one-dimensional atmospheric model presented here uses a two-stream approximation. It uses a radiative code with a convective adjustment coupled with a chemistry code to determine the temperature-pressure structure of an atmosphere. See Chapter 3 for a detailed breakdown of the equations used.

Our model begins by determining the equilibrium chemistry of the atmosphere in question. An initial estimation of the temperature and pressure structure is required, but it need not be accurate because the model is iterative and will recalculate chemistry in the future. Chemical equilibrium is determined using the publically-available Chemical Equilibrium with Applications (CEA), a NASA code that minimizes Gibbs free energy (see Section 3.2.3 for more details). CEA takes initial chemical compositions and determines the equilibrium compositions at the input temperature and pressure.

The chemical composition of the atmosphere determines the frequency-dependent optical depth of the atmosphere. Optical depth is a function of opacity, as shown in Equation 2.7 and opacity of the atmosphere is calculated using absorption cross-sections from Molliere *et al.* (2015).

Once frequency-dependent optical depth has been determined, the radiative transfer through the atmosphere can be solved. This is done iteratively, by determining the downcoming and upgoing radiation at each point in the atmosphere and adjusting the local temperature until the atmosphere reaches radiative equilibrium when net radiation at each point in the atmosphere reaches zero. Once the temperature structure of the atmosphere is established, the pressure structure is recalculated using the hydrostatic balance equation, Equation 2.3.

Once the temperature-pressure structure of the atmosphere in radiative and hydrostatic equilibrium has been determined, the convective adjustment is applied. Every point in the atmosphere is checked to determine if it violates the Schwarzchild criterion (Equation 2.13), making the atmosphere at that location unstable and inducing convection. If convection occurs, the temperature change as a function of altitude is adjusted to follow the atmosphere's adiabatic lapse rate, $\frac{dT}{dz} = \frac{-g}{c_p}$. After the convective adjustment is applied, the radiative transfer code is run again to ensure that radiative equilibrium is not violated in the sections of the atmosphere that are not under the influence of convection.

The new radiative-convective temperature-pressure structure is fed into the chemical code, chemical equilibrium is determined at these temperatures and pressures and the entire process starts again, with the chemical code, radiative transfer and convective adjustment being reapplied until the atmosphere's temperature and pressure structure converges.

2.2.4 Validation tests

A number of tests were performed to ensure that the model described in Section 2.2.3 was capable of producing reliable and valid results.

Grey atmosphere tests

This model was first tested using a grey, or frequency-independent, atmosphere. Tests were performed for early Earth, modern Earth and modern Mars and compared to the known (or estimated, in the case of early Earth) temperature-pressure structures. Because this model splits the atmosphere into layers allowing for the resolution of the temperature-pressure structure to be changed, each test was run with a range of resolution, proving that the results shown are independent of the setup of the problem.

When the atmosphere has reached equilibrium, the net flux at each level of the atmosphere is zero and the flux leaving the top of the atmosphere is equal to the stellar flux entering the atmosphere. Testing was also performed for the limiting case of a planet with no atmosphere to prove that the model would produce the correct surface temperature (i.e. equilibrium temperature) for the planet.

Figure 2.2 shows the comparison between Earth and Mars models and data. To generate this plot, it was assumed that all incoming radiation was in the visual band, and all outgoing radiation was in the infrared, and that the opacity in the visual band was zero, or that no incoming radiation was absorbed, as per Pierrehumbert (2010). For the outgoing radiation, the opacity of Mars's atmosphere was taken from Badescu (2010), who calculated the Rosseland mean opacities for carbon dioxide at various temperatures and pressures. Because the Rosseland mean opacity for air was not readily available (available mean opacities are for temperatures far hotter than Earth's), the opacity of Earth's atmosphere was calculated using Earth's average surface optical depth of 0.7 (Fowler, 2007) and back-calculating the opacity using Equation 2.7.

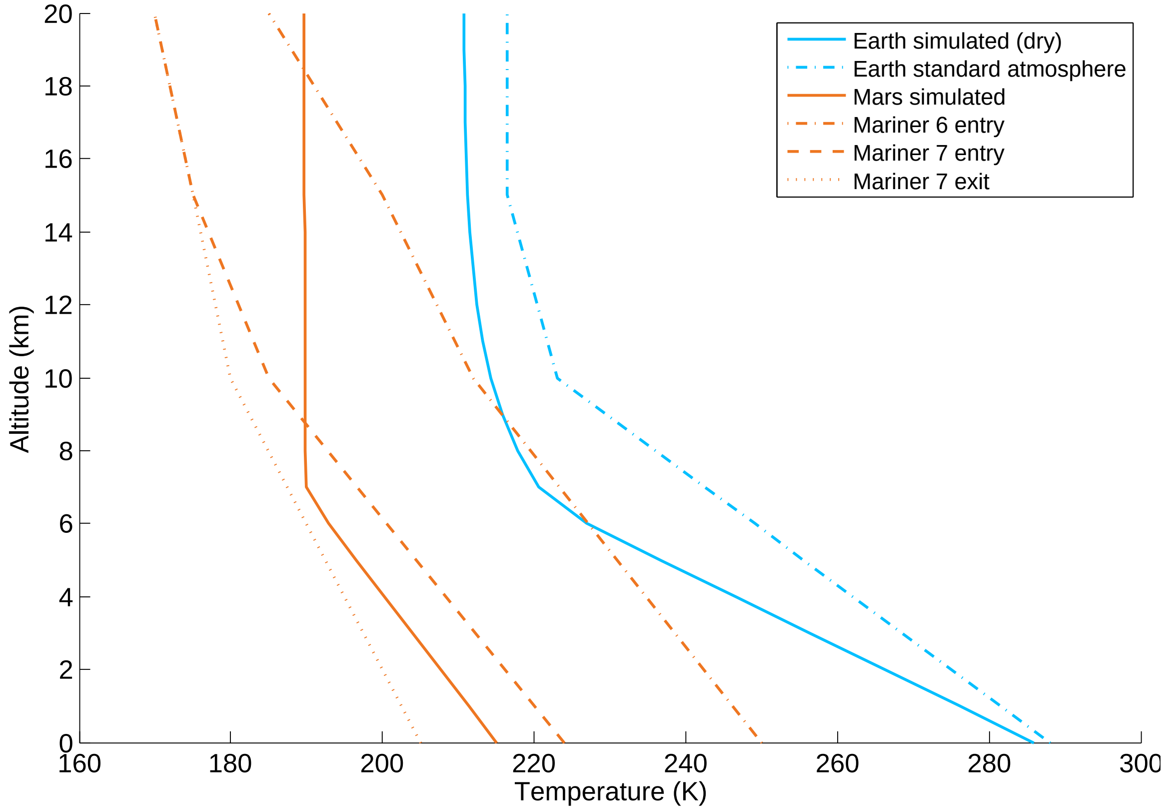

Figure 2.2: Comparison between modelled and actual atmospheric temperature for Earth and Mars. Earth actual data is from the US Standard Atmosphere (NASA, 1976) and Mars actual data is from the Mariner 6 and 7 missions (Rasool *et al.*, 1970). Near the surface, the Mariner data is accurate to ± 5K, while towards the top of the plot, the data is accurate to ± 20K.

Because this model uses a dry convective lapse rate, and Earth's true convective lapse rate is moist, the temperature in the lower part of the atmosphere drops more quickly in the modelled data than in the real atmosphere, giving the temperature in the lower atmosphere a shallower profile than expected.

Figure 2.3 shows the comparison between radiative-only and radiative-convective models in Earth's atmosphere, using both the dry convective lapse rate of the atmosphere (standard for this model) and the moist convective lapse rate. This figure illustrates how convection cools the planet surface and increase the temperature of the atmosphere above it.

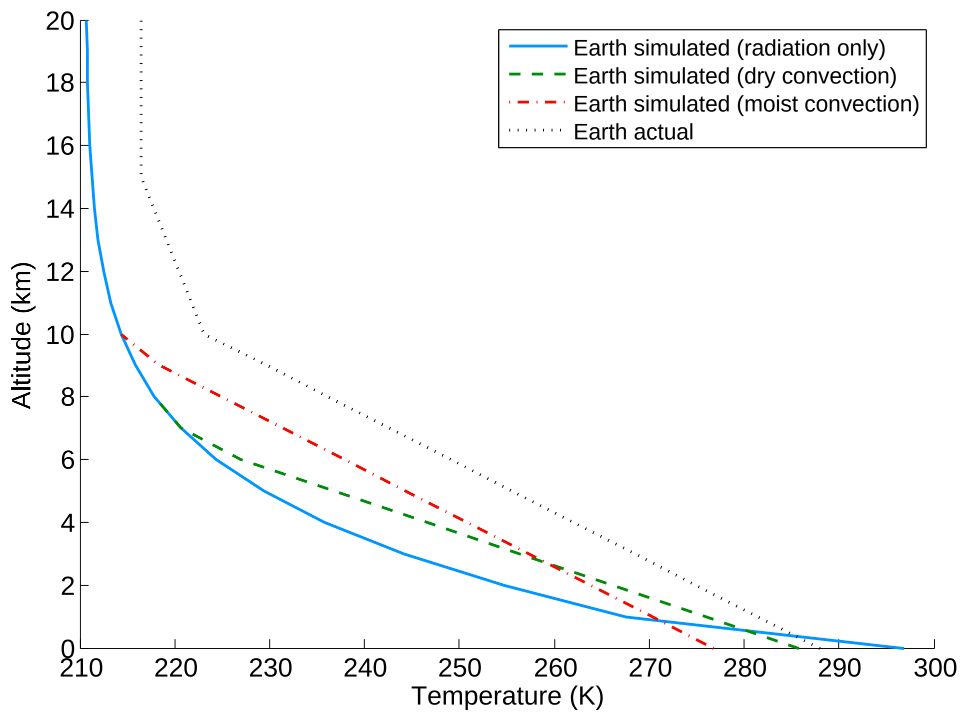

Figure 2.3: Comparison between modelled and actual atmospheric temperature for Earth, with dry convection and moist convection in the lower atmosphere. Earth actual data is from the US Standard Atmosphere (NASA, 1976).

A brief note on Venus: as the other terrestrial planet with an atmosphere in our solar system, it would seem reasonable to model its atmosphere as a test for this code. However, Venus's atmosphere behaves differently than Mars's or Earth's, and presents difficulties that the other two planets do not. While Venus's albedo is very high in the visual (about 0.7) and it reflects the majority of the visual radiation it receives, its albedo drops significantly in the UV band, to about 0.25. This means that it does not reflect in the UV. The SO_2 clouds in Venus's atmosphere, plus an unknown UV absorber, absorb large amounts of radiation. The clouds then re-emit that UV radiation in infrared and this is what heats the planet's surface (Titov *et al.*, 2013). Thus, due to its heavy cloud cover that converts UV radiation to infrared, the radiative transfer in Venus's atmosphere is heavily frequency-dependent in a way that the radiative transfer in Earth's and Mars's atmospheres are not, so it cannot be modelled using a grey atmosphere model.

Multifrequency tests

Once it was established that the model performed well in calculating the temperature-pressure structures for grey atmospheres, frequency dependence was implemented. This was done both to determine that the code gave the appropriate results with frequency-dependence implemented and to determine the time it takes to run frequency-dependent tests. This was necessary because increasing the number of frequencies increased the computation time, but reducing the number of frequencies had the potential of smoothing over frequency-dependent changes in the atmosphere's opacity.

Table 2.1 shows the results of tests using atmospheres with a range of number of layers and number of frequencies, along with the flux going into the atmosphere and exiting it. So that the test conditions were kept consistent, if the frequency fell into the infrared, it was given an opacity of $9*10^{-5}$, consistent with a surface optical depth of 0.7 (Earth's optical depth, Fowler (2007)) and if it fell into the visual band, it was given an opacity of zero. This simulates the presence of a greenhouse gas like carbon dioxide or water that absorbs only in the infrared. The run times shown in this table were for the program run on a laptop with a single CPU. Incoming and outgoing flux are at the top of the atmosphere, while the surface temperature is the temperature calculated by the radiative code.

In addition to showing the independence of results to changing problem setup, this table shows the dependence of run time on the number of layers and frequencies. With the exception of the grey code, which is significantly faster because it does not have to step through frequency space, this dependence is linear: a ten-fold increase in number of frequencies causes a ten-fold increase in time, and a five-fold increase in number of layers causes a five-fold increase in time.

It should be noted that, due to the simplicity of the frequency dependence (i.e. opacities were one of two values), this model converged very quickly. Using opacity data derived from absorption cross-sections, as described in Section 3.2.4, can cause the code to take significantly longer to converge. See Section 3.2.4 for testing using opacities derived from absorption cross-sections.

Table 2.1: Comparing grey and multifrequency results

Test	Incoming flux (W/m^2)	Outgoing flux (W/m^2)	T_{surf} (K) (radiative)	Run time (s)
Grey, 10 layers	340.3	339.0	295.8	0.14
Grey, 50 layers	340.3	338.9	296.2	0.33
Grey, 100 layers	340.3	338.9	296.2	0.56
Grey, 1000 layers	340.3	338.9	296.2	4.5
10 stream, 10 layers	340.3	338.9	297.5	9.8
10 stream, 50 layers	340.3	338.9	297.9	44.9
100 stream, 10 layers	340.3	338.9	295.8	88.7
100 stream, 50 layers	340.3	338.9	296.2	436.0
1000 stream, 10 layers	340.4	340.8	296.3	806.5
1000 stream, 50 layers	340.4	340.8	296.1	4321.6

2.3 Conclusions

At its core, the modelling of an atmosphere requires the treatment of atmospheric chemistry, through equilibrium or disequilibrium models, and the treatmet of energy transfer through the atmosphere, through radiation and convection in a one-dimensional model, and through radiation, convection and winds in a three-dimensional model.

The principles outlined in this chapter provide a primer on atmospheric physics and the principles of atmospheric modelling. These are the basis for the code described in Chapter 3.

Chapter 3

Super-Earth atmospheres based on formation history, with applications to the TRAPPIST-1 system

3.1 Introduction

Super-Earths, planets up to ten times Earth's mass, are considered the most likely type of planet to be habitable. Super-Earths are the most abundant class of exoplanet observed (Howard *et al.*, 2011), and, at the time of writing, 52 of the observed Super-Earths orbit within the habitable zone of their host star (Laboratory, 2017). Of particular interest for this thesis, it was recently discovered that TRAPPIST-1, an ultracool M-dwarf, hosts seven of these such planets, with between three and five of the planets orbiting within the star's habitable zone (Gillon *et al.*, 2017). The potential habitability of the TRAPPIST-1 system, determined through atmospheric modelling, is the focus of this chapter.

For a planet to be habitable, it needs to be temperate, have a surface, and have an atmosphere. These conditions allow the planet to host liquid water on its surface, which is generally considered necessary for life.

As evidenced by our own solar system where Venus's thick atmosphere makes it inhospitable, Earth's moderate atmosphere readily supports life and Mars's thin atmosphere allows the planet to freeze, atmospheres can have a dramatic effect on a planet's surface conditions, and are thus an important factor in determining the potential habitability of a planet.

An atmosphere's composition has a large impact on the planet's surface conditions: atmospheres made of molecules that absorb in the infrared, like water and carbon dioxide, will cause hotter surface conditions than an atmosphere of the same mass but composed of molecules that absorb in other bands, like nitrogen, oxygen or hydrogen. This is due to the fact that, for temperate planets, the atmosphere and the surface of the planet itself emit radiation that peaks in infrared. If the atmosphere can reabsorb that infrared radiation, the planet experiences a greenhouse effect, with the amount of heating due to the greenhouse effect a function of the number of infrared absorbing molecules in the atmosphere.

A planet's atmosphere can be formed through accretion of gas from the protoplanetary disc in which the planet forms, through outgassing of volatiles from the planet's core, or from a combination of these methods (Forget and Leconte, 2014).

The species accreted onto the planet, in either gas or solid form, depend on the formation history of the planet, both in terms of the planet's migration and where in the disc the planet formed. Cridland *et al.* (2016) and Cridland *et al.* (2017) model gas accretion onto planets throughout their migration through a protoplanetary disc and the track species found in planet atmospheres for planets formed in a variety of locations. Alessi *et al.* (2017) model the abundance of solids found in the cores of planets based on their formation history, and Elkins-Tanton and Seager (2008) and Schaefer and Fegley Jr. (2009) model outgassing of volatiles from solid cores to determine the composition of outgassed atmospheres. We use the results of these studies to guide the compositions we select for our models of the TRAPPIST-1 system, seen in Section 3.4.

This chapter describes the atmosphere model created (Section 3.2), discusses atmosphere formation (Section 3.3), and applies the model created to the TRAPPIST-1 system (Section 3.4).

3.2 Model

The model developed uses a one-dimensional radiative-convective code, written in Matlab, coupled with a chemistry code to determine the variation of atmospheric temperature with pressure.

3.2.1 Radiative code

The radiative code used employs a one-dimensional plane-parallel approximation. This approximation allows the atmosphere to be modeled without having to consider spherical co-ordinates by modeling it as a slab of gas extending from the surface of the planet upwards towards space.

Further, radiation is modeled using a two-stream approximation, as per Ramanthan and Coakley Jr. (1978) and Pierrehumbert (2010). This approximation assumes that all incoming (downgoing, I_-) radiation enters the atmosphere at a fixed angle, and all outgoing (upcoming, I_+) radiation exits the atmosphere at a fixed angle. Each stream can be configured as a single frequency independent stream or as many frequency dependent streams all travelling in the same direction.

To solve the radiative code, the atmosphere is separated into layers that are in hydrostatic balance, and the upcoming and downgoing fluxes are calculated at each layer using Equations 3.1 and 3.2. Each layer in the atmosphere is assumed to emit thermally. Following the method outlined by Pierrehumbert (2010), optical depth, τ_ν, is zero at the bottom of the atmosphere and increases with height, reaching $\tau_{\infty,\nu}$ at the top of the atmosphere.

$$I_+(\nu,\tau_\nu) = I_+(\nu,0)e^{-\tau_\nu} + \int_0^{\tau_\nu} \pi B(\nu,T(\tau_\nu^{'}))e^{-(\tau_\nu-\tau_\nu^{'})}d\tau_\nu^{'} \tag{3.1}$$

$$I_-(\nu,\tau_\nu) = I_-(\nu,\tau_{\infty,\nu})e^{-(\tau_{\infty,\nu}-\tau_\nu)} + \int_{\tau_\nu}^{\tau_{\infty,\nu}} \pi B(\nu,T(\tau_\nu^{'}))e^{-(\tau_\nu^{'}-\tau_\nu)}d\tau_\nu^{'} \tag{3.2}$$

Flux hitting the top of the atmosphere is simply blackbody radiation from the host star scaled by distance and divided by 4 to account for the fact that, while the stellar flux falls onto only one face of the planet, with an area of πR^2, the rotation of the planet spreads the received energy over its entire surface area of $4\pi R^2$.

$$I_-(\nu, \tau_{\infty,\nu}) = \frac{\pi}{4}\frac{R_{star}^2}{d^2}B(\nu, T_{star}) \tag{3.3}$$

Radiation leaving the planet's surface is comprised both of radiation reflected by the surface due to the planet's albedo and radiation emitted from the surface. The radiation reflected by the planetary albedo is assumed to reflect at the same frequency it hit the surface, leaving the spectrum of radiation unchanged. The radiation emitted from the surface is the radiation emitted by a blackbody at the equilibrium temperature of the planet. This second part provides a boundary condition for the code.

The planet's equilibrium temperature is calculated from its host star's temperature, distance to the host star, and planet albedo.

$$T_{eq} = T_{star}(1-a)^{1/4}\sqrt{\frac{R_{star}}{2D}} \tag{3.4}$$

The upcoming flux from the surface is thus simply the sum of the reflected flux and the blackbody flux from the planet itself.

$$I_+(\nu, 0) = \pi B(\nu, T_{eq}) + aI_-(\nu, 0) \tag{3.5}$$

Equations 3.1 and 3.2 are integrated over frequency to find total flux at each layer in the atmosphere, as shown in Equation 3.6. Note the shift from indexing with optical depth to indexing with altitude: in order to calculate flux and temperature of an atmosphere, the flux must be calculated at the same physical location at every frequency. Because optical depth is frequency-dependent, leading to a single physical location having a range of optical depths depending on the frequency, altitude is used for indexing instead.

$$I(\tau(z)) = \int I(\nu, \tau_\nu(z))d\nu \tag{3.6}$$

To find the temperature of the atmosphere, a time-stepping method is used. An initial guess of the temperature structure of the atmosphere is chosen (this guess need not be realistic (Ramanthan and Coakley Jr., 1978), and the net radiative heating rate of each layer, $\frac{dT_0(\tau)}{dt}$ is calculated. The net radiative heating rate is given by Equation 3.7 (Ramanthan and Coakley Jr., 1978) where g is the gravitational acceleration, c_p is the atmosphere's specific heat at constant pressure, $\Delta I(\tau)$ is the flux at the top of the layer minus the flux at the bottom of the layer, and ΔP is the pressure at the top of the layer minus the pressure at the bottom of the layer.

$$\frac{dT_0(\tau)}{dt} = \frac{g}{c_p}\Big[\frac{\Delta I_-(\tau)}{\Delta P} - \frac{\Delta I_+(\tau)}{\Delta P}\Big] \tag{3.7}$$

The temperature at the next time step $t_1 = t_0 + \Delta t$ is calculated using Equation 3.8.

$$T_1(\tau) = T_0(\tau) + \frac{dT_0(\tau)}{dt}\Delta t \tag{3.8}$$

This new temperature profile is used to calculate the new fluxes and heating rates, and this code is iterated until the system reaches equilibrium when $\frac{dT_0(\tau)}{dt}$ goes to zero.

At equilibrium, the net flux at all points in the atmosphere must be zero, which occurs when $\Big[\frac{\Delta I_-(\tau)}{\Delta P} - \frac{\Delta I_+(\tau)}{\Delta P}\Big]$ goes to zero. This requirement yields a boundary condition at the surface of the planet, which allows the planet's surface temperature to be calculated. This is expressed in Equation 3.9, where σT_{eq}^4 is the blackbody radiation emitted at the planet's equilibrium temperature, $I_-(0)$ is the radiation exiting the bottom of the atmosphere and $I_-(\tau_\infty)$ is the radiation from the star hitting the top of the atmosphere. This equation essentially says that the surface temperature of the planet must be such that the planet emits as much flux as it absorbs: the planet absorbs σT_{eq}^4 from the star, and also absorbs radiation emitted from the atmosphere, given by $I_-(0) - I_-(\tau_\infty)$.

$$T_{surf} = \Big(\frac{\sigma T_{eq}^4 + I_-(0) - I_-(\tau_\infty)}{\sigma}\Big)^{1/4} \tag{3.9}$$

3.2.2 Convective code

Typically, on planets with thin atmospheres and solid surfaces, convection is expected to occur in the lower regions of the atmosphere. This is because the surface of the planet absorbs more radiation than the atmosphere, which leads to a temperature discontinuity between the planet's cooler atmosphere and its hotter surface (Seager, 2010). This temperature discontinuity drives convection.

Convection has the effect of modifying the temperature structure of the atmosphere. A radiative-only model tends to over-estimate a planet's surface temperature and underestimate the temperature higher in the atmosphere (Manabe and Strickler, 1964), leading to large temperature gradients in the lower atmosphere. The maximum temperature gradient of the atmosphere is dictated by the convective lapse rate: an atmosphere cannot have a temperature gradient higher than the convective lapse rate. If an atmosphere does have a lapse rate higher than allowed by the convective lapse rate, vertical fluid motion is induced, which redistributes the heat in the atmosphere so the lapse rate falls to the convective lapse rate.

Thus, when modelling atmospheres, if the radiative code produces a temperature gradient larger than allowed by the convective lapse rate, then the temperature gradient is recalculated to follow the convective lapse rate.

The stability of the atmosphere to convection is determined using the Schwarzchild criterion: if $-\frac{dT}{dz} < \frac{g}{c_p}$, where g is the gravitational acceleration at the planet's surface and c_p is the heat capacity at constant pressure of the atmosphere, then the planet's atmosphere is unstable and convection occurs. The temperature gradient of the atmosphere is then given by the convective lapse rate, which is assumed to be dry adiabatic lapse rate, as per Ramanthan and Coakley Jr. (1978) and Pierrehumbert (2010), and is calculated using Equation 3.10.

$$\frac{dT}{dz} = -\frac{g}{c_p} \tag{3.10}$$

Convection is implemented in the radiative-convective code by first allowing the atmosphere to reach radiative equilibrium, then determining which regions of the atmosphere have temperature gradients greater than allowed by the convective lapse rate. In the regions where convection occurs, the temperature is adjusted such that it follows the lapse rate, with the temperature of the convective layer being determined by the lapse rate and the temperature of the layer below it. For example, if the surface temperature is sufficient to drive convection, then the temperature of the layer above the planet's surface is given by $T = T_{surf} - \frac{g}{c_p} d_{layer}$, where d_{layer} is the thickness of the layer.

For equilibrium to be maintained in the atmosphere, the net flux at the top of the convective region must remain equal to that calculated in the radiative-only model

(Manabe and Strickler, 1964). To ensure this is true, the convective adjustment is allowed to lower the surface temperature, which lowers the temperature of each layer above it, reducing the upgoing flux back to its radiation-only value. The lowering of the planet's surface temperature has physical meaning, since, in real planets, convection cools the planet's surface (Manabe and Strickler, 1964).

3.2.3 Chemistry code

In this model, it is assumed that the atmosphere is in local chemical equilibrium at every point in the atmosphere. This is the simplest way to handle atmospheric chemistry, is customary in the modelling of exoplanet atmospheres (Beuther *et al.*, 2014), and provides a good starting place for atmospheric modelling. See Section 2.1.4 for a discussion on chemical equilibrium and disequilibrium.

Atmospheric chemistry is modelled using NASA's publically-available Chemical Equilibrium with Applications (CEA) (Gordon and McBride (1994); McBride and Gordon (1994)), a chemical equilibrium code that calculates equilibrium compositions of mixtures by minimizing Gibbs free energy for a given temperature and pressure. CEA also outputs the density and the specific heat of the mixture which are used to calculate the pressure structure and convective adjustment of the atmosphere respectively.

Initial atmospheric chemical compositions are taken from planet formation and outgassing models (see Sections 3.3.1 and 3.3.2) and these initial compositions are run through the CEA program to find the actual compositions of the atmospheres.

3.2.4 Calculating opacities

The opacity of a planet's atmosphere dictates how much radiation is absorbed by the atmosphere. Opacity is proportional to the absorption cross-section, which is a property of the atmosphere's chemical composition, temperature and pressure, and the absorption cross-section of molecules in the atmosphere must be modified to account for broadening. In general, broadening has the effect of causing the atmosphere to be more opaque than expected, and is induced through three main processes: natural broadening, Doppler broadening and pressure broadening (Carroll and Ostlie, 2007). Natural broadening is simply a consequence of the fact that a spectral line cannot be infinitely thin, Doppler broadening is broadening due to the movement of molecules in a gas which causes the frequencies of light emitted or absorbed by the atmosphere to be Doppler-shifted, and pressure broadening is due to the perturbation of orbitals in an atom from interactions with another atom or ion (Carroll and Ostlie, 2007).

Each of these effects must be taken into account when determining the true absorption cross-section of a molecule in an atmosphere. The absorption cross-sections used in this chapter were calculated first by Molliere *et al.* (2015) with an expanded range of temperatures and pressures calculated by Molliére that will be available to the public in the future. They used raw data from the Exomol (Tennyson *et al.*, 2016), HITEMP (Rothman *et al.*, 2013) and Kurucz (Kurucz, 1993) databases, which provide unbroadened absorption cross-sections for a variety of molecules, and applied broadening corrections to these pre-calculated cross-sections.

The frequency-dependent opacity of the atmosphere, κ_ν can be calculated using Equation 3.11, where σ_ν is the frequency-dependent absorption cross-section and m is the mass of a molecule of the gas that makes up the atmosphere (Carroll and Ostlie, 2007). Because absorption cross-section is dependent on atmospheric temperature and pressure, opacity of the atmosphere changes as a function of altitude.

$$\kappa_\nu = \frac{\sigma_\nu}{m} \tag{3.11}$$

If multiple gases are present in the atmosphere, the total opacity of the atmosphere may be determined by simply doing a sum of opacities, weighted by the concentration of the gases present. This is shown in Equation 3.12, where $\kappa_{\nu,i}$ is the opacity of each gas and q_i is the mass-specific concentration of each gas. The concentration of each gas can change as a function of altitude should the chemical composition of the atmosphere change (Pierrehumbert, 2010).

$$\kappa_\nu = \sum_{i=0}^{n} \kappa_{\nu,i} q_i \tag{3.12}$$

To use opacity, it must be converted to optical depth. The frequency-dependent optical depth of the atmosphere, $\tau_\nu(z)$, can then be calculated using Equation 3.13, where g is the planet's gravity, P_0 is the planet's surface pressure and $P(z)$ is the atmospheric pressure at altitude z (Pierrehumbert, 2010).

$$\tau_\nu(z) = \frac{-2}{g} \int_{P0}^{P(z)} \kappa_\nu(z) dP \tag{3.13}$$

This optical depth is then used in the calculation of flux through the atmosphere, shown in Equations 3.1 and 3.2. To handle the frequency-dependence of the optical depth, a line-by-line approach is used, where flux is calculated at numerous frequencies and integrated to find net flux at each level of the atmosphere. The effect of resolution in frequency can be seen below.

Dependency of results on frequency resolution

In Section 2.2.4 it was established that results of the code presented here were independent of problem setup. With that established, the first test for the frequency dependent model was to determine how many frequencies should be used: frequency dependence is implemented using a line-by-line approach so infinitely many frequencies could, in theory, be used.

Frequency dependence is implemented using data from Molliere *et al.* (2015), who provided the absorption cross-sections for molecules as a function of frequency, temperature and pressure. Each data file from Molliere *et al.* (2015) includes over 7 million entries, where each entry contains a single frequency and its corresponding absorption cross-section. Each data file is for a fixed temperature and pressure and data files are available for temperatures and pressures ranging from 81 K to 3000 K and 10^{-5} bar to 10^{3} bar. All told, when selecting only temperatures and pressures expected for the TRAPPIST-1 planets, this is roughly 10 GB of information per molecule.

To properly model an atmosphere, which varies in both temperature and pressure, multiple data files must be used. This is further complicated if more than one molecule is used to make up the atmosphere, since each data file only contains information for a single molecule.

From this data, four subsamples of different sizes, made through sampling every n entries, were extracted. The four values of n were 7000, 1000, 100, and 10, which created subsamples with approximately 1000, 7000, 70000 and 700000 entries respectively.

The atmosphere of TRAPPIST-1 d was modelled using the subsamples with 1000 and 7000 entries (see Section 3.5 for the results of this modelling). There is little difference between the two models: the difference in surface temperature is only 1.2 K, and, with the exception of the top of the atmosphere, which has a temperature difference of up to 5.7 K, the rest of the temperature profile is within 1.5 K from model to model.

Ideally, this should be tested using the 70000 and 700000 line files. However, due to the constraints of running these tests on a laptop (the 1000 line test took 8 hours to converge, and the 7000 hour test took 6 hours when starting with the converged result from the 1000 line test, and both tests used 95-100% of CPU capacity the entire time), further tests with more entries are saved for future work and runs done supercomputers.

3.2.5 Integration of model components

Modelling an atmosphere using this code is iterative. The code takes an initial guess of the temperature and pressure structure (which need not be realistic) and calculates the initial hydrostatic balance of the atmosphere. It then takes atmospheric chemical composition and the initial pressure-temperature structure and uses CEA to determine the chemical equilibrium and specific heat of the atmosphere. Opacities for the atmosphere are determined using absorption cross-sections from Molliere *et al.* (2015). The atmospheric composition and opacities are passed into the radiative equilibrium code which iterates to convergence. A convective adjustment is applied where necessary and the code checks that radiative equilibrium in the rest of the atmosphere is not violated. The hydrostatic and chemical equilibria are recalculated using updated temperature and pressure conditions and the updated chemistry is resubmitted to the radiative code. This entire process is run until convergence. This is shown schematically in Figure 3.1.

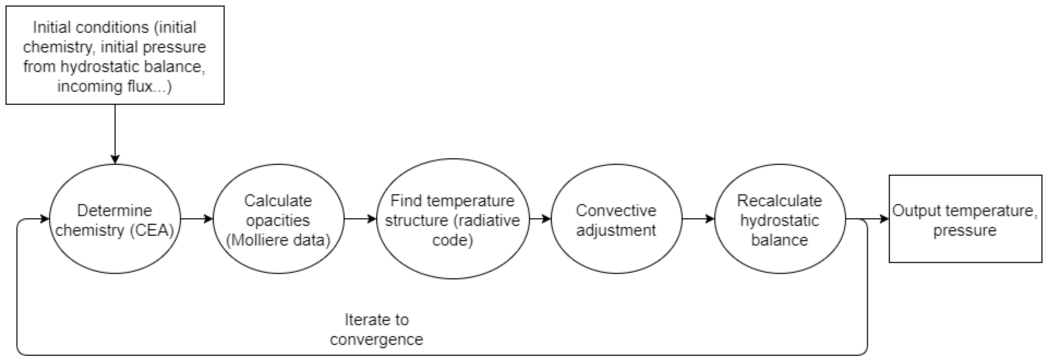

Figure 3.1: Schematic of the integration of all model components

3.2.6 Limitations to this model

This model assumes the atmosphere experiences absorption only, so does not account for the effects of scattering (see Section 2.2.2 for a full discussion on the effects of scattering and reasons for keeping this model absorption-only). This means that effects of clouds in the atmosphere cannot be accounted for.

Additionally, because this model is one-dimensional, it cannot account for three-dimensional effects such as high winds that could be found if the planets are tidally locked. It also does not account for non-equilibrium chemistry, including photochemistry, which can impact the planet's atmospheric chemistry. However, at this point, very little is known about the composition of many terrestrial exoplanets, including the TRAPPIST-1 system, so this model provides a starting point to estimate potential atmospheres with the potential to integrate elements like photochemistry and tidal heating in the future.

3.3 Formation of Atmospheres

Atmospheres can be formed through accretion of gas from the protoplanetary disc or through outgassing of volatiles from the planet core. The following subsections discuss the method of formation and the resulting atmospheric compositions from each formation pathway.

3.3.1 Accreted atmospheres

The composition of an atmosphere formed through accretion of gas from the protoplanetary disc depends on the composition of gas in the protoplanetary disc. Since the composition of the protoplanetary disc changes as a function of radial position, atmospheric composition depends on the location of the planet's formation and its subsequent migration.

Cridland *et al.* (2016) and Cridland *et al.* (2017) model the composition of accreted atmospheres on planets with different formation and migration histories. They use the concept of planet traps, inhomogeneities in the protoplanetary disc where planets slow their migration and accrete large amounts of solids and gas, and identify three key traps, the water ice line trap, heat transition trap and dead zone trap. Table 3.1 shows the trace gases accreted onto the planet core for planets with different formation histories. These trace gases react with one another to form the planet's atmospheric composition, a process described in Section 3.4.2.

Table 3.1: Minor gas abundance as a percentage of mass not in H_2 and He (Table 5, Cridland *et al.* (2016))

	Dead zone (%)	Ice line (%)	Heat transition (%)
H_2O	99.84	67.92	61.15
CO	< 0.01	30.40	36.70
H	< 0.01	0.02	0.1
CO_2	< 0.01	0.32	0.09
N_2	< 0.01	< 0.01	1.85
NH_3	< 0.01	0.69	< 0.01
HCN	0.12	0.2	< 0.01
CH_4	< 0.01	0.45	0.11
HNC	0.02	< 0.01	< 0.01

3.3.2 Purely outgassed atmospheres

As with accreted atmospheres, the composition of outgassed atmospheres depends on the planet's formation and migration history, which dictates which solids (including their accompanying volatiles) are accreted into the planet core. The volatiles in the planet core are then outgassed through impact or volcanism (Forget and Leconte, 2014).

Alessi *et al.* (2017) model the solid composition of planets based on their formation and migration history. Like Cridland *et al.* (2016) and Cridland *et al.* (2017), they use the concept of planet traps, where planets slow their migration and accrete large amounts of material. Compositions of planets formed in each trap are shown in Table 3.2.

The volatiles found in these planets can be outgassed to form planetary atmospheres. Elkins-Tanton and Seager (2008) and Schaefer and Fegley Jr. (2009) model outgassed atmospheres of terrestrial planets and identify the range in composition

Table 3.2: Solid composition of planets formed in different traps in the protoplanetary disc (Alessi *et al.*, 2017), with the TRAPPIST-1 planets that could form in each trap identified. Percents are percent mass.

	Cosmic ray dead zone (%) (CRDZ)	Ice line (%) (IL)	Heat transition (%) (HT)
Ices	5.9	30.9	47.7
Mantle	53.9	39.6	30.1
Core	40.2	29.5	22.2
Potential planets	c, d	d, e	f

that is possible. Both Elkins-Tanton and Seager (2008) and Schaefer and Fegley Jr. (2009) use meteorite types in their outgassing models, identifying which volatiles are released from each meteorite type. Examples of outgassed atmospheres can be seen in Table 3.4.

3.4 TRAPPIST-1 system

With seven closely packed terrestrial planets, and up to five planets orbiting in the star's habitable zone, the TRAPPIST-1 system is both an interesting system for future observations and important in the search for life outside our solar system.

3.4.1 The case for TRAPPIST-1 as habitable

The TRAPPIST-1 system is a promising system in the search for life because it has between three and five potentially Earth-like planets orbiting within the star's habitable zone, depending on how the habitable zone is calculated. This both increases the chance of a planet with Earth-like surface conditions being found around

TRAPPIST-1 and allows future observations to observe multiple planets in one mission. Parameters of the four most promising planets are listed in Table 3.3.

Table 3.3: Properties of potentially-habitable TRAPPIST-1 planets (data from Gillon *et al.* (2017))

Planet	c	d	e	f
Radius (R_{Earth})	1.056 ± 0.035	0.772 ± 0.030	0.918 ± 0.039	1.045 ± 0.038
Mass (M_{Earth})	1.38 ± 0.61	0.41 ± 0.27	0.62 ± 0.58	0.68 ± 0.18
Density (ρ_{Earth})	1.17 ± 0.53	0.89 ± 0.60	0.80 ± 0.76	0.60 ± 0.17
Equilibrium temperature (K) (Bond albedo 0)	341.9 ± 6.6	288.0 ± 5.6	251.3 ± 4.9	219.0 ± 4.2
Equilibrium temperature (K) (Bond albedo 0.3)	313.0 ± 9.2	263.7 ± 8.1	230.0 ± 7.3	200.4 ± 6.8
Equilibrium temperature (K) (Bond albedo 0.7)	253.3 ± 7.4	213.3 ± 6.6	186.1 ± 7.3	162.2 ± 5.5

Life as we know it requires liquid water, and the ability of a planet to hold liquid water on its surface is dependent on the planet's atmosphere. There is some debate as to whether or not planets orbiting M-dwarves in the star's habitable zone are capable of retaining their atmospheres: the M-dwarf's active nature has the potential to strip atmospheres from the planet's surface, leaving behind the rocky core and rendering these planets inhospitable. Studies have been performed on both sides of the argument, with Wheatley *et al.* (2017) showing that planets in the TRAPPIST-1 system could lose their entire atmosphere over 3 billion years, and Garraffo *et al.* (2016) showing a similar result for Proxima b, the rocky planet orbiting M-dwarf Proxima Centauri, while Barnes *et al.* (2016) show that the presence of a magnetic field could protect an atmosphere of a planet orbiting an M-dwarf, and Wheatley *et al.* (2017) notes that their model is simplistic and the upper limit to mass loss.

However, as mentioned in Section 1.1.1, TRAPPIST-1 b and c were observed to have atmospheres (de Wit *et al.*, 2016). These atmospheres have a featureless spectrum for each planet, ruling out cloud-free hydrogen-dominated atmospheres, but allowing for H_20, CO_2, N_2 or O_2 dominated atmospheres. The presence of atmospheres on the two inner TRAPPIST-1 planets is a promising indication that atmospheres on planets d, e and f, located further from the host star and thus subject to lower rates of atmospheric erosion, are also possible.

Migration plays a role in the retention of a planet's atmosphere: Wheatley *et al.* (2017) show that an atmosphere could be protected through planet migration where the planet forms in the outer reaches of the protoplanetary disc and migrates inwards as the star ages, staying away from the star during the star's active youth. Unterborn *et al.* (2017) shows that the close packing of the TRAPPIST-1 system is likely the product of migration, with the planets are located at 1/8 to 1/2 of their starting distance to the star.

Additionally, with the exception of planet c, the planets in the TRAPPIST-1 system are all less dense than Earth (see Table 3.3), which suggests that reservoirs of volatiles could exist in the planets' cores, which could replenish atmosphere loss as it occured (Burgasser and Mamajek, 2017).

Finally, TRAPPIST-1 b and c are not the only terrestrial planets orbiting M-dwarves to have observed atmospheres: two of the only three well-constrained Super-Earth atmospheric observations belong to planets orbiting M-dwarves. GJ 1132 b, a planet of 1.6 Earth masses, orbits inside the inner limit of its star's habitable zone, making it subject to higher levels of stellar irradiation than a planet in the star's habitable zone. It has been observed to have a thick atmosphere that is likely made of methane and water (Southworth *et al.*, 2016). GJ 1214 b, a planet of 6.55 Earth masses, also orbits within the inner limit of its star's habitable zone, and also has a thick atmosphere, likely made predominantly of water (Berta *et al.*, 2011).

While the majority of the potentially-habitable planets in the TRAPPIST-1 system have had no atmospheric observations at this point, these points make it reasonable to expect that all the potentially habitable planets in the TRAPPIST-1 system might retain atmospheres.

However, the presence of an atmosphere does not automatically render a planet hospitable, and surface conditions must be calculated based on the atmosphere composition and incoming radiation from the host star. The following sections thus present possible atmospheres on the planets in the TRAPPIST-1 system with the intention of determining which atmospheres yield temperate surface conditions.

3.4.2 Modelling atmospheres on the TRAPPIST-1 planets

Unterborn *et al.* (2017) model the composition of TRAPPIST-1 b through g, and estimate where each planet formed the protoplanetary disc relative to the disc's water ice line. They indicate that planets f and g are extremely volatile-rich, being roughly 50% water by weight, so likely formed outside of the water ice line of the disc, while planets b and c are rocky (∼6-8% water by weight) and formed inside the ice line. Planets d and e are less well-constrained, with d possibly having similar compositions to planets b and c, and e falling somewhere in between c and f.

Unterborn *et al.* (2017)'s results help constrain the possible atmospheres that could be found on the TRAPPIST-1 planets. Due to the planets' likely formation locations, it can be assumed that, if the TRAPPIST-1 planets formed atmospheres through accretion, planets f and g are more likely to have atmospheres like those accreted by Cridland *et al.* (2016) and Cridland *et al.* (2017)'s dead zone or ice line planets, planets b and c are more likely to have atmospheres formed in the heat transition region, and planets d and e could have atmospheres of any of these types. These atmospheric compositions can be seen in Table 3.5.

If, however, the atmospheres were formed through outgassing, it is assumed for the purposes of this work that, given the similarities of the TRAPPIST-1 planets to those modelled by Alessi *et al.* (2017) (see Table 3.2), planets b and c were formed in the star's cosmic ray dead zone trap, and planets f and g were formed in the star's heat transition trap. Because their composition is not well constrained, planets d and e could have formed in any trap.

Because the formation history of the TRAPPIST-1 system and true meteoritic composition is unknown, a range of possible atmospheres is chosen. These atmospheric compositions and likely meteoritic compositions are outlined in Table 3.4. The likely meteoritic compositions are derived from results of Schaefer and Fegley Jr. (2009), who show which volatiles are outgassed for each meteorite type by modelling outgassing from planetesimals made of chondritic meteorites (carbonaceous chondrites, or CI, CM and CV, ordinary chondrites, or H, L and LL, and enstatite chondrites, or EH and EL). It is assumed that all hydrogen and helium that was outgassed (present in outgassed volatiles from ordinary chondrites Schaefer and Fegley Jr. (2009)) has escaped, leaving only heavier elements behind. See Appendix A for a calculation of thermal escape.

Regardless of the origin of the planet's atmosphere, some processing must be done before the temperature-pressure structure of the atmosphere can be determined. Because both the accreted atmospheres and outgassed atmosphere models (shown

Table 3.4: Initial composition of outgassed atmospheres 300 K and 1 atm (101325 Pa), with the planets in the TRAPPIST-1 system that could host these atmospheres identified.

Composition	%	Planet trap	Potential planet	Constituent meteorite type
H_2O	100	HT	f	CI/CM
H_2O CO_2	70/80/90 30/20/10	HT, IL	d, e, f	CI/CM/CV
H_2O CO	50/65 50/35	IL	d, e	H/L/LL
CO CO_2	70/90 30/10	CRDZ	c, d	EL/EH

in Sections 3.3.1 and 3.3.2 respectively) yield only initial chemical abundances for the atmospheres, these compositions must be run through CEA to determine the atmosphere's equilibrium chemical composition.

Examples of chemical compositions of the atmospheres being modelled are shown in Table 3.5, which shows compositions of accreted atmospheres, and Table 3.7, which shows compositions of outgassed atmospheres. In both tables, the potentially habitable planets in the TRAPPIST-1 system on which these atmospheres might form are identified. The compositions seen in these tables are the chemical equilibrium compositions of Tables 3.1 and 3.4.

In the accreted atmospheres case (Table 3.1), equilibrium chemistry was run both with only the trace species shown in Table 3.1 and with these trace species plus an abundance of hydrogen and helium. The first case follows the assumption that only the heavier trace species were accreted onto the planet, while the second case assumes that hydrogen and helium were accreted and interacted with the trace species.

The accretion of hydrogen and helium to the planet's core impacts the composition of the atmospheres: rather than carbon monoxide breaking apart to form carbon dioxide, it instead breaks apart to combine with the excess hydrogen to form water and methane. Likewise, nitrogen, which stays in its molecular form in the absence of hydrogen, bonds with hydrogen, creating ammonia. These are shown in Table 3.6.

In the case where hydrogen and helium were allowed to accrete and react with the trace species, it was assumed that, after reacting with the trace species, all hydrogen and helium escaped through thermal escape, leaving only the trace species and heavier products behind. For the smallest planet, TRAPPIST-1 d, it is also likely that any substantial amount of methane in its atmosphere would be lost through thermal escape, while methane could be retained on the larger planets. See Appendix A for the calculation of thermal escape.

Of note, when run to equilibrium, carbon monoxide in the planet atmospheres bonds with water and formed carbon dioxide and solid carbon in cases where there was no excess hydrogen for the carbon to bond with. However, in cases where there was excess hydrogen available, this carbon bonds with it to form methane. Thus, the presence or lack of excess hydrogen impacts the type of species that might be accreted into an atmosphere.

In the case where solid carbon was formed, it was assumed that the solid carbon, shown as C_{gr} in Tables 3.5, 3.6 and 3.7, rains out to the surface and became part of the core. Additionally, it is assumed that liquid or frozen water remained suspended in the atmosphere, as it does on Earth, rather than all raining out to the surface.

The formation of solid carbon and its subsequent fall to the planet's surface has the effect of lowering the atmosphere's C/O ratio from equal to that of the accreted gas or the outgassed gas to something lower. The change in the C/O ratio varies depending on the initial composition and final equilibrium composition, but can be as high as a factor of two (e.g. a pure CO atmosphere equilibrates to a pure CO_2 atmosphere, lowering the C/O ratio from 1 to 0.5). This means that one cannot assume that a atmosphere's observed C/O ratio has any correlation to the C/O ratio of the protoplanetary disc in which the planet formed.

Table 3.5: Accreted atmosphere equilibrium compositions at 300 K and 1 atm (101325 Pa) and the planets on which these atmospheres could potentially be found. Percents are percent mass

	X-ray dead zone (%)	Ice line (%)	Heat transition (%)
H_2O	99.86	77.20	71.40
CO_2	0	9.60	12.92
N_2	0.05	0.47	1.36
CH_4	0.02	0	0
C_{gr}	0.07	12.73	14.32
Potential planets	d, e, f	d, e, f	c, d, e

Table 3.6: Accreted atmosphere equilibrium compositions at 300 K and 1 atm (101325 Pa) accreted with excess hydrogen and the planets on which these atmospheres could potentially be found. Percents are percent mass

	X-ray dead zone (%)	Ice line (%)	Heat transition(%)
H_2O	99.81	80.54	76.43
CO_2	0	0	0
N_2	0	0	0
NH_3	0.09	0.79	2.15
CH_4	0.09	18.66	21.42
C_{gr}	0	0	0
Potential planets	e, f	e, f	c, e

As can be seen in Tables 3.5 through 3.7, there is a degeneracy in atmospheric

Table 3.7: Equilibrium composition of outgassed atmospheres at 300 K and 1 atm (101325 Pa), with the planets in the TRAPPIST-1 system that could host these atmospheres identified

Initial composition	%	Equilibrium composition	%	Potential planet
H_2O	100	H_2O	100	f
H_2O	70/90	H_2O	85.07/95.65	d, e, f
CO_2	30/10	CO_2	14.93/4.35	
H_2O	50/65	H_2O	60.86/74.28	d, e
CO	50/35	CO_2	19.57/12.86	
		$C_{(gr)}$	19.57/12.86	
CO	70/90	CO_2	60.72/53.30	c, d
CO_2	30/10	$C_{(gr)}$	39.28/46.70	

compositions among many of the cases shown. Thus, for the purposes of modelling, these cases are combined.

Table 3.8, a consolidation of Tables 3.5 through 3.7, shows the list of atmospheric compositions that are to be tested along with the planets on which these atmospheres might be found. The planet trap column indicates where an atmosphere of this type may have formed: HT is the heat transition trap, DZ is the dead zone trap and IL is the ice line trap. Outgassed and accreted indicate whether the atmosphere was formed through outgassing of solids or through accretion of gas from the protoplanetary disc. Excess H_2 indicates that the atmospheres were run to chemical equilibrium in the presence of hydrogen, as per Table 3.6.

The temperature and pressure structure of atmospheres with the above abundances are to be calculated for atmospheres with surface pressures ranging from 1000 Pa to 10 MPa. 1000 Pa was chosen as the lower limit for surface pressures because water cannot exist in a liquid form at pressures much below this point. Albedo is to be varied from 0.2 to 0.7.

Table 3.8: Possible atmospheric compositions of the TRAPPIST-1 planets. Percents are percent mass

Initial composition	%	Planet trap	Potential planet
H_2O	100	Outgassed HT, accreted DZ	f
CO_2	100	Outgassed DZ	c,d
H_2O CO_2	70/90 30/10	Outgassed HT, outgassed IL, accreted HT, accreted IL	d, e, f
H_2O CH_4	80 20	Accreted IL (excess H_2)	c,e,f
H_2O CH_4 NH_3	78 20 2	Accreted IL (excess H_2)	c,e

3.5 Results: TRAPPIST-1 atmosphere models

Due to time constraints, only one atmosphere was modelled: a 100 % CO_2 atmosphere on planet d. This corresponds to an outgassed CO/CO_2 atmosphere where, in equilibrium, all of the CO was broken and rebonded into CO_2 and $C_{(gr)}$. It was assumed that all $C_{(gr)}$ rained out of the atmosphere.

For this test, planetary albedo was set at 0.3 and surface pressure at 10^5 Pa, or roughly Earth-like conditions. 25 atmosphere layers were used because this spacial resolution yielded good convergence. Future atmosphere models with different compositions and for the other TRAPPIST-1 planets are shown in Table 3.8 and described in Chapter 4.

Figure 3.2 shows the temperature and pressure structure found using this model. An interesting feature can be seen with this atmosphere: because the TRAPPIST-1 star is an M-dwarf and thus emits primarily in infrared radiation, and CO_2 absorbs primarily in infrared, the atmosphere absorbs a large amount of incoming radiation,

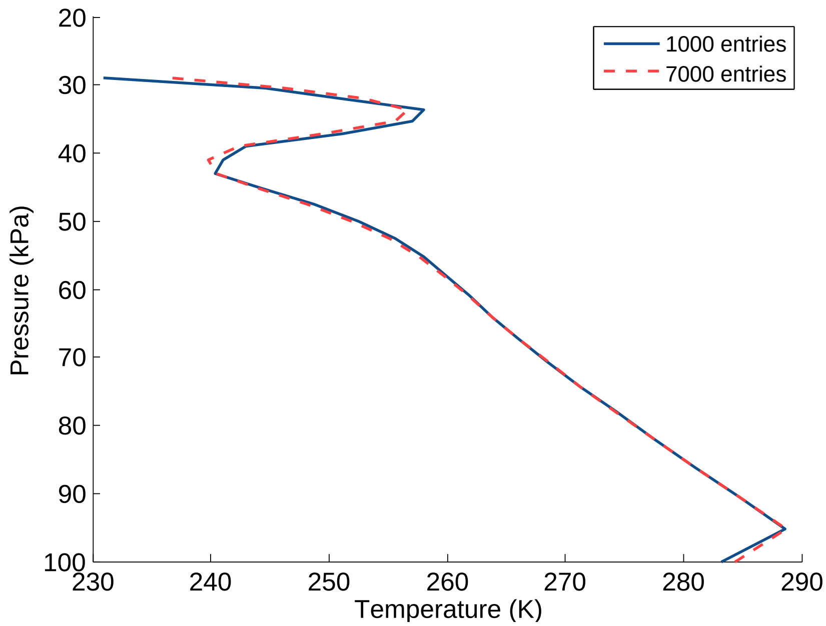

(a) Temperature and pressure structure

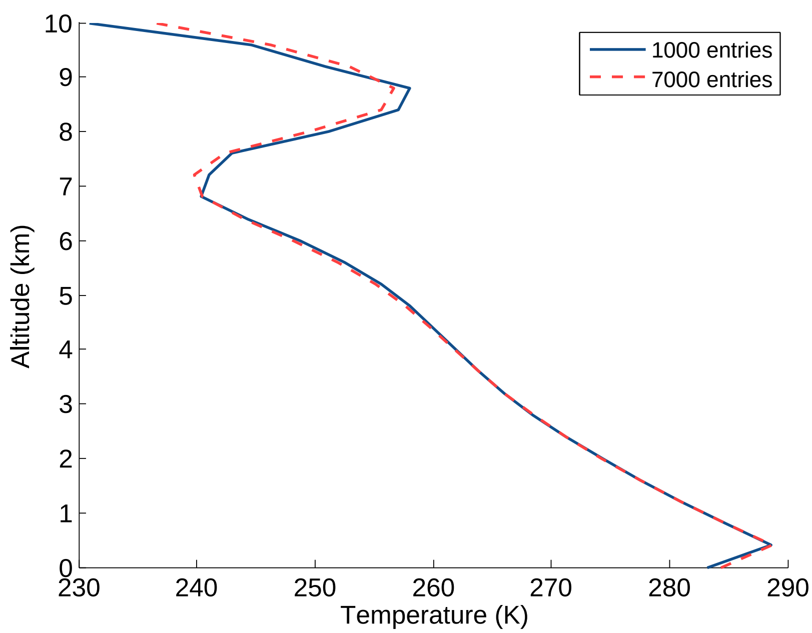

(b) Temperature as a function of altitude

Figure 3.2: Temperature structure for a 100% CO_2 atmosphere on TRAPPIST-1 d

and the top of the atmosphere heats up. This is similar to the ozone layer in Earth's atmosphere, which absorbed UV radiation and causes the atmosphere around it to increase in temperature.

The inversion in the lower part of the atmosphere is an artifact of the radiative-only modelling and will be smoothed out when the convective adjustment is applied in future models.

The TRAPPIST-1 d atmosphere is relatively warm through its entirety, again due to the fact that all of the radiation that the atmosphere is exposed to is infrared, and the atmosphere absorbs in the infrared.

3.6 Discussion

These initial results show that the atmospheres of planets orbiting cool stars behave differently than the atmospheres in our own system. Because cool stars emit in the infrared, a planet orbiting a cool star with an atmosphere that contains a greenhouse gas like water vapour or carbon dioxide will absorb some of the incoming stellar radiation in addition to infrared radiation leaving the planet's surface, whereas a planet orbiting a sunlike star absorbs infrared radiation only from the planet's surface. This absorption of incoming infrared radiation creates a temperature inversion not seen in other work: models like those by Morley *et al.* (2017) assume the TRAPPIST-1 atmospheres behave like Earth's own atmosphere in which the absorption of incoming radiation can be neglected.

It should be noted that these results are still preliminary and the assumptions in this model have some effect on the results.

This model assumed that the atmosphere was in chemical equilibrium. However, planetary atmospheres often are subject to non-equilibrium effects like photochemistry (Morley *et al.*, 2017). For example, Earth's own ozone layer is a product of photodissociation of oxygen molecules by UV radiation.

In addition to creating species like ozone that could be observed (see Section 3.6.1), photodissociation can destroy molecules that equilibrium chemistry indicates could be present and observable. Ammonia, specifically, is readily dissociated in planetary atmospheres (Morley *et al.*, 2017), so can be expected to be lost in the TRAPPIST-1 planets.

This model uses a cloud-free two-stream approximation which calculates the average temperature and pressure structure of the atmosphere. If, however, the atmosphere is very cloudy, scattering of radiation is no longer negligible, which can impact the atmosphere's temperature-pressure structure. Forget and Pierrehumbert (1997) show that carbon dioxide clouds on early Mars could scatter infrared radiation coming from the planet's surface, warming the planet in a scattering variant of the greenhouse effect. The amount of impact that this would have on a planet that also receives infrared radiation from its host star has not yet been modelled, but it is certainly an effect that should be considered.

3.6.1 Observing TRAPPIST-1 atmospheres

Due to the degeneracy in atmospheric compositions from different planet and atmospheric formation history (discussed in Section 3.4.2), it is likely not possible to determine a Super-Earth's planet or atmosphere formation history through observations. However, observations will determine the atmospheric composition which is important in constraining the planet's surface temperature.

Because the TRAPPIST-1 planets are small, with likely relatively thin atmospheres, atmospheric observation is challenging but feasible. As mentioned in Section 1.1.1, TRAPPIST-1 b and c had their atmospheres observed in a combined spectrum using the Hubble Space Telescope (HST) in 2016 (de Wit *et al.*, 2016) and were found to have atmospheres that produced a featureless spectrum.

This rules out cloud-free hydrogen-dominated atmospheres but leaves the possibility open for H_2O, CO_2, N_2 or O_2 dominated atmospheres, which would also produce a featureless spectrum. Figure 3.3 shows the HST observations of TRAPPIST-1 b and c.

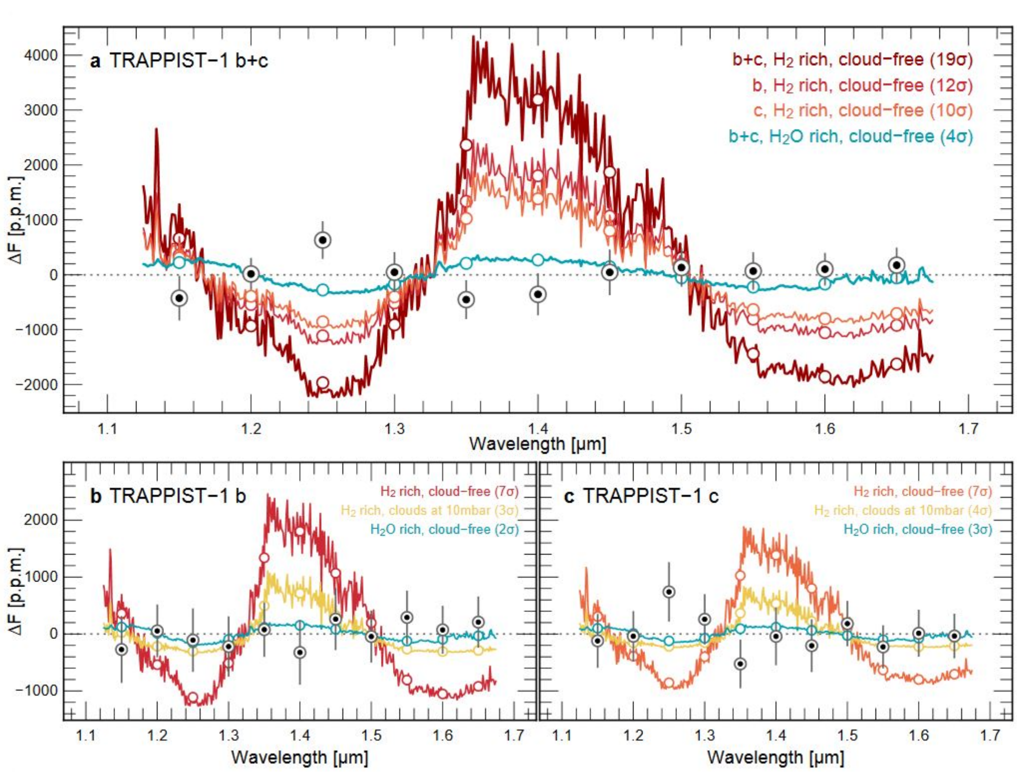

Figure 3.3: Observations of TRAPPIST-1 b and c compared with theoretical predictions (Figure 3, (de Wit *et al.*, 2016)).

However, the Hubble Space Telescope is not capable of observing detailed spectra of small exoplanets, and detailed observations of the TRAPPIST-1 system's atmospheres must be taken using James Webb Space Telescope (JWST) or a ground-based telescope like the European Extremely Large Telescope (ELT) (de Wit *et al.*, 2016). Because the ELT and other extremely large telescopes like it are not slated for first light until the mid-2020s, the most promising source of observations of the TRAPPIST-1 system is JWST.

Barstow and Irwin (2016) show that JWST would be capable of detecting present-day Earth levels of ozone on the TRAPPIST-1 planets, and Batalha (2016) (see Figure 1.5 in Section 1.1.1) shows that JWST is capable of observing all of the molecules shown in Table 3.8.

Additionally, Morley *et al.* (2017) show that JWST would be capable of observing carbon dioxide atmospheres on all TRAPPIST-1 planets. Provided that the atmospheres had surface pressures greater than 0.1 bar, these observations could be performed using fewer than 100 transits, with some planets requiring significantly fewer transits: they predict the atmosphere of TRAPPIST-1 e being determined in as few as 4 eclipses.

3.7 Conclusions

This chapter presents a one-dimensional chemistry-dependent radiative-convective model that is designed to be used to model the atmospheres of terrestrial planets. This model is frequency-dependent, and, provided one has correct absorption cross-sections, can be used to model any atmospheric composition. When using frequency-dependent cross-sections, the model is perhaps best suited for use on a dedicated computer or a supercomputer, because, even when using only 1000 frequencies, it monopolizes the entire CPU capacity of a laptop for upwards of 8 hours.

This model was used to begin modelling atmospheres for the TRAPPIST-1 system. The initial compositions of the TRAPPIST-1 atmospheres were modelled from planet formation history models, and both atmospheres formed through accretion and outgassing were considered. While the method of formation of atmospheres through outgassing differs substantially from the method of formation from accretion, many of the resulting atmospheres have similar compositions. It is thus likely not possible to distinguish the source of a terrestrial atmosphere based solely on its composition.

Additionally, the chemical reactions within the atmosphere after its formation can drive the atmosphere's C/O ratio away from that of the protoplanetary disc in which it formed. Thus, observations of an atmosphere's C/O ratio cannot be relied on to inform observers about the formation of the planet.

Results of the initial modelling of an atmosphere on TRAPPIST-1 d reveal that temperature inversions and warm upper atmospheres are to be expected in these atmospheres: the planet's host star emits primarily in the infrared, which is readily absorbed by gases like CO_2 as it enters the atmosphere. This is a new result that has not been seen before in other atmosphere models.

Chapter 4

Future Work

Due to the fact that the absorption cross-section data from Molliere *et al.* (2015) were not available until very late in the writing of this thesis, the majority of tests for the TRAPPIST-1 system must still be run. Given the computing power necessary, these will be run on a supercomputer, which will significantly decrease the time it takes for a test to be run, allowing a wide range of atmospheric compositions to be tested.

Table 4.1 shows the atmospheric compositions to be run. These will be run for surface pressures of 10^3 Pa, 10^5 Pa and 10^7 Pa, with albedos of 0.15 (Mars-like: rocky with little to no water), 0.3 (Earth-like: mix of water and land) and 0.7 (icy planet, or planet with substantial clouds).

With the completion of these models, an array of atmospheres based on planet formation will be created. At this point, no such array exists. This array of atmospheres can be compared with future atmospheric observations to help determine the surface conditions of the TRAPPIST-1 planets.

Table 4.1: Future models to be run for the TRAPPIST-1 planets. Percents are percent mass.

Initial composition	%	Potential planet
H_2O	100	f
CO_2	100	c,d
H_2O	70/90	d, e, f
CO_2	30/10	
H_2O	80	c,e,f
CH_4	20	
H_2O	78	c,e
CH_4	20	
NH_3	2	

Chapter 5

Conclusions

This thesis presents a code to model atmospheres of exoplanets, with a particular focus on modelling atmospheres on potentially-habitable exoplanets. This code combines a frequency-dependent radiative-convective code with an equilibrium chemistry code to determine the temperature-pressure structure of a planet's atmosphere.

The code was tested for both grey and frequency-dependent atmospheres, and initial models were created for TRAPPIST-1 d using a database of opacities from Molliere *et al.* (2015).

Possible atmospheric compositions for planets in the TRAPPIST-1 system, a likely primary target of JWST, are presented. These compositions are based on formation history and are modelled for both accreted atmospheres and outgassed atmospheres. Of note, when these initial atmospheric compositions chemically equilibrate, their C/O ratio can change: for example, an atmosphere that is initially made up of carbon monoxide will re-bond to form carbon dioxide and granular carbon. It is assumed that this granular carbon rains out to the ground, leaving the atmosphere with less carbon than it had in its initial composition, and lowering the C/O ratio of the atmosphere.

This has the consequence that observations of atmospheric C/O ratios cannot be relied on to provide information about the initial composition of the atmosphere, and thus the initial composition of the protoplanetary disc in which the planet formed.

Initial models for the TRAPPIST-1 atmospheres indicate that atmospheres on planets orbiting cool stars are heated in a different way than atmospheres in our own solar system. In our own solar system, the sun's radiation peaks in the visual band, with negligible emission in the infrared, so greenhouse gases in an atmosphere absorb infrared radiation emitted from the planet's surface only. On the contrary, an atmosphere containing greenhouse gases on a planet orbiting a cool star will absorb infrared radiation both from the incoming stellar radiation and the outgoing radiation emitted by the planet's surface, heating the upper part of the atmosphere and potentially creating temperature inversions.

In the future, more atmospheres on planets in the TRAPPIST-1 system will be modelled with varying compositions, surface pressures and albedos to develop a database of possible atmospheres that can then be compared with observations from future missions like JWST to help determine which surface conditions are likely on these potentially-habitable planets.

Appendix A

Mass loss in atmospheres

Even in the absence of other forms of atmospheric erosion, like heating from XUV radiation or stellar winds, thermal escape is sufficient to cause the loss of hydrogen and helium in the TRAPPIST-1 planets' atmospheres.

Thermal escape, or Jeans escape, occurs when the high-velocity tail of the Maxwell-Boltzmann distribution is larger than the escape velocity of the planet. The most probable velocity, given a Maxwell-Boltzmann distribution, is given by Equation A.1, where k is the Boltzmann constant, T is the temperature of the atmosphere, usually taken to be the temperature of the exosphere because that is where molecules escape, and m is the molar mass of atmosphere (Coates, 2017).

$$v_0 = \sqrt{\frac{2kT}{m}} \tag{A.1}$$

Escape velocity can be calculated using Equation A.2, where z is the altitude of escape (Coates, 2017).

$$v_{esc} = \sqrt{\frac{2GM_{planet}}{R_{planet} + z}} \tag{A.2}$$

The escape flux Φ, or the number of molecules leaving the atmosphere per unit area per second, can be calculated using Equation A.3, where $n(z)$ is the number density of the atmosphere, v_{esc} is the escape velocity of the planet, and v_0 is the most probable velocity given the planet's atmospheric temperature, assuming a Maxwell-Boltzmann distribution (Coates, 2017).

$$\Phi = \frac{n(z)v_0}{2\sqrt{\pi}}\Big(\frac{v_{esc}^2}{v_0^2} + 1\Big)exp\Big(-\frac{v_{esc}^2}{v_0^2}\Big) \tag{A.3}$$

Table A.1 shows the escape flux for various types of atmospheres. All atmospheres were calculated using a number density of $0.025*10^{-27}$, which is equal to that of an ideal gas at Earth's surface temperature and pressure and a temperature of 1000 K, the temperature expected in planet exospheres. Escape flux was calculated for both the smallest potentially-habitable TRAPPIST-1 planet (planet d, radius of 0.772 R_{Earth} and mass of 0.41 M_{Earth}) and the largest (planet c, radius of 1.056 R_{Earth} and mass of 1.38 M_{Earth}). As a point of reference, escape flux for air leaving Earth is $1.4*10^{-57}$ molec/sec/m^2 and for carbon dioxide leaving Mars is $3.2*10^2$ molec/sec/m^2. This table shows that, in both cases, hydrogen and helium are lost at rates 20 orders of magnitude greater than the loss rate of Mars's atmosphere and up to 83 orders of magnitude greater than the loss rate of Earth's atmosphere, while carbon monoxide, carbon dioxide, water and oxygen all have loss rates less than that seen on Mars, indicating that atmospheres of these molecules would remain on planets in the TRAPPIST-1 system. On planet c, however, a methane-dominated atmosphere could be lost.

The timescale for hydrogen and helium escape is very rapid: assuming a pure hydrogen atmosphere with a mass of 10^{18} kg (the same order of magnitude as Earth's), the entire atmosphere would be lost in a matter of months to years. Likewise, helium escapes over a matter of years to ten of years. An estimation for this escape timescale, T, is shown in Equation A.4, where A is the surface area of the planet, taken to be 10^{12} m^2, M is the mass of the planet atmosphere, taken to be 10^{18} kg, m is the mass of the molecule in question and Φ is the escape flux, shown in Table A.1.

$$T = \frac{M}{\Phi m A} = \frac{10^{18}}{10^{26} * 10{-}27 * 10^{12}} = 10^7 \ sec = 115 \ days \tag{A.4}$$

Table A.1: Escape fluxes for various atmospheres

Composition	Escape flux, planet d (molec/sec/m^2)	Escape flux, planet c (molec/sec/m^2)
H_2	1.3*10^{26}	5.2*10^{21}
He	1.3*10^{23}	9.5*10^{13}
CO	1.7*10^{-14}	7.6*10^{-81}
CO_2	3.0*10^{-39}	9.4*10^{-144}
H_2O	4.8*10^{1}	1.5*10^{-41}
CH_4	5.8*10^{4}	1.0*10^{-33}
O_2	1.1*10^{-20}	1.4*10^{-96}

Bibliography

Alessi, M., Pudritz, R., and Cridland, A. (2017). Composition of Early Planetary Atmospheres II: Coupled Dust and Chemical Evolution in Protoplanetary Disks. *MNRAS*, **464**(1).

Anglada-Escudé, G., Amado, P. J., Barnes, J., Berdiñas, Z. M., Butler, R. P., Coleman, G. A. L., de La Cueva, I., Dreizler, S., Endl, M., Giesers, B., Jeffers, S. V., Jenkins, J. S., Jones, H. R. A., Kiraga, M., Kürster, M., López-González, M. J., Marvin, C. J., Morales, N., Morin, J., Nelson, R. P., Ortiz, J. L., Ofir, A., Paardekooper, S.-J., Reiners, A., Rodríguez, E., Rodríguez-López, C., Sarmiento, L. F., Strachan, J. P., Tsapras, Y., Tuomi, M., and Zechmeister, M. (2016). A terrestrial planet candidate in a temperate orbit around Proxima Centauri. *Nature*, **536**, 437–440.

Arney, G., Meadows, V., Domagal-Goldman, S., Deming, D., Robinson, T., Tovar, G., Wolf, E., and Schwieterman, E. (2017). Pale Orange Dots: the Impact of Organic Haze on the Habitability and Detectability of Earthlike Exoplanets. *ApJ*, **836**(49).

Badescu, V. (2010). Tables of Rosseland mean opacities for candidate atmospheres of life hosting free-floating planets. *Central European Journal of Physics*, **8**(3).

Barnes, R., Dietrick, R., Luger, R., Driscoll, P., Quinn, T., Fleming, D., Guyer, B., McDonald, D., Meadows, V., Arney, G., Crisp, D., Domagal-Coldman, S., Lincowski, A., Lustig-Yaeger, J., and Schwieterman, E. (2016). The Habitability of Proxima Centauri b I: Evolutionary Scenarios. *ArXiv e-prints*, (1608.06919).

Barstow, J. and Irwin, P. (2016). Habitable worlds with JWST: transit spectroscopy of the TRAPPIST-1 system? *MNRAS*, **461**(1).

Batalha, N. (2016). ERES II Graduate workshop, Cornell University.

Berta, Z., Charbonneau, D., Désert, J.-M., Miller-Ricci Kempton, E., McCullough, P., Burke, C., Fortney, J., Irwin, J., Nutzman, P., and Homeier, D. (2011). The Flat Transmission Spectrum of the Super-Earth GJ1214B from Wide Field Camera 3 on the Hubble Space Telescope. *ApJ*, **747**(35).

Beuther, H., Klessen, R., Dullemond, C., and Henning, T., editors (2014). *Protostars and Planets VI*. University of Arizona Press.

Burgasser, A. and Mamajek, E. (2017). On the Age of the TRAPPIST-1 system. *ArXiv e-prints*, (1706.02018).

Carroll, B. and Ostlie, D. (2007). *An Introduction to Modern Astrophysics*. Pearson.

Charbonneau, D., Berta, Z. K., Irwin, J., Burke, C. J., Nutzman, P., Buchhave, L. A., Lovis, C., Bonfils, X., Latham, D. W., Udry, S., Murray-Clay, R. A., Holman, M. J., Falco, E. E., Winn, J. N., Queloz, D., Pepe, F., Mayor, M., Delfosse, X., and Forveille, T. (2009). A super-Earth transiting a nearby low-mass star. *Nature*, **462**(7275).

Clampin, M., Valenti, J., Deming, D., and Group, J. S. W. (2007). Detection of Planetary Transits with the James Webb Space Telescope. *ExoPTF Whitepaper*.

Coates, A. (2017). *Atmospheric escape*. Mullard Space Science Laboratory, UCL, UK.

Cridland, A., Pudritz, R., and Alessi, M. (2016). Composition of Early Planetary Atmospheres I: Connecting Disk Astrochemistry to the Formation of Planetary Atmosphere. *MNRAS*, **461**(3).

Cridland, A., Pudritz, R., Birnstiel, T., Cleeves, L., and Bergin, E. (2017). Composition of Early Planetary Atmospheres II: Coupled Dust and Chemical Evolution in Protoplanetary Disks. *MNRAS*, **469**(4).

de Wit, J., Wakeford, H. R., Gillon, M., Lewis, N. K., Valenti, J. A., Demory, B.-O., Burgasser, A. J., Burdanov, A., Delrez, L., Jehin, E., Lederer, S. M., Queloz, D., Triaud, A. H. M. J., and Van Grootel, V. (2016). A combined transmission spectrum of the Earth-sized exoplanets TRAPPIST-1 b and c. *Nature*, **537**, 69–72.

Elkins-Tanton, L. and Seager, S. (2008). Ranges of Atmospheric Mass and Composition of Super-Earth Exoplanets. *ApJ*, **685**(2).

Forget, F. and Leconte, J. (2014). Possible Climates on Terrestrial Exoplanets. *Proc. of. the Royal Society A*, **372**(2014).

Forget, F. and Pierrehumbert, R. (1997). Warming Early Mars with Carbon Dioxide Clouds that Scatter Infrared Radiation. *Science*, **278**(5341).

Fowler, A. (2007). *Climate Dynamics*. University of Limerick, UK.

Garraffo, C., Drake, J., and Cohen, O. (2016). The Space Weather of Proxima Centauri b. *ApJ*, **1**(L4).

Gillon, M., Triaud, A. H. M. J., Demory, B.-O., Jehin, E., Agol, E., Deck, K. M., Lederer, S. M., de Wit, J., Burdanov, A., Ingalls, J. G., Bolmont, E., Leconte, J., Raymond, S. N., Selsis, F., Turbet, M., Barkaoui, K., Burgasser, A., Burleigh, M. R., Carey, S. J., Chaushev, A., Copperwheat, C. M., Delrez, L., Fernandes, C. S., Holdsworth, D. L., Kotze, E. J., Van Grootel, V., Almleaky, Y., Benkhaldoun, Z., Magain, P., and Queloz, D. (2017). Seven temperate terrestrial planets around the nearby ultracool dward star TRAPPIST-1. *Nature*, **542**, 456–460.

Gordon, S. and McBride, B. (1994). *Computer Program for Calculation of Complex Chemical Equilibrium Compositions and Applications. Part 1: Analysis*. NASA, National Aeronautics and Space Administration,Washington, D.C. 20546-0001, USA.

Han, E., Wang, S. X., Wright, J. T., Feng, Y. K., Zhao, M., Fakhouri, O., Brown, J. I., and Hancock, C. (2017). Exoplanet Orbit Database. II. Updates to Exoplanets.org. *Publications of the Astronomical Society of the Pacific*, **126**, 827.

Hasegawa, Y. and Pudritz, R. (2011). The origin of planetary system architectures - I. Multiple planet traps in gaseous discs. *MNRAS*, **417**(2).

Howard, A., Marcy, G., Bryson, S., Jenkins, J., Rowe, J., Batalha, N., Borucki, W., Koch, D., Dunham, E., and Gautier III, T. (2011). Planet Occurence within 0.25 AU of Solar-Type Stars from Kepler. *ApJ*, **201**(2).

Howard, A., Sanchis-Ojeda, R., Marcy, G., Johnson, J., Winn, J., Isaacson, H., Fischer, D., Fulton, B., Sinukoff, E., and Fortney, J. (2013). A Rocky Composition for an Earth-sized Exoplanet. *Nature*, **503**, 381384.

Jimenez-Aquino, J. and Varela, J. (2005). Two stream approximation to radiative transfer equation: An alternative method of solution. *Revista Mexicana Defisica*, **51**(1).

Kasting, J., Pollack, J., and Ackerman, T. (1984). Response of Earth's Atmosphere to Increases in Solar Flux and Implications for Loss of Water from Venus. *Icarus*, **57**(3).

Kasting, J., Whitmire, D., and Reynolds, R. (1993). Habitable zones around main sequence stars. *Icarus*, **101**(1).

Kempton, E. (2010). The properties of super-Earth atmospheres. *Proc. IAU. Symp. No. 276.*

Kipping, D. M., Cameron, C., Hartman, J. D., Davenport, J. R. A., Matthews, J. M., Sasselov, D., Rowe, J., Siverd, R. J., Chen, J., Sandford, E., Bakos, G. Á., Jordán, A., Bayliss, D., Henning, T., Mancini, L., Penev, K., Csubry, Z., Bhatti, W., Da Silva Bento, J., Guenther, D. B., Kuschnig, R., Moffat, A. F. J., Rucinski, S. M., and Weiss, W. W. (2017). No Conclusive Evidence for Transits of Prixima b in MOST photometry. *ApJ*, **153**(3).

Kurucz, R. (1993). *SYNTHE Spectrum Synthesis Programs and Line Data.* Cambridge, Mass.: Smithsonian Astrophysical Observatory.

Laboratory, P. H. (2017). Habitable Exoplanets Catalogue. University of Puerto Rico at Arecibo.

Luger, R., Sestovic, M., Kruse, E., Grimm, S. L., Demory, B.-O., Agol, E., Bolmont, E., Fabrycky, D., Fernandes, C. S., Van Grootel, V., Burgasser, A., Gillon, M., Ingalls, J. G., Jehin, E., Raymond, S. N., Selsis, F., Triaud, A. H. M. J., Barclay, T., Barentsen, G., Howell, S. B., Delrez, L., de Wit, J., Foreman-Mackey, D., Holdsworth, D. L., Leconte, J., Lederer, S., Turbet, M., Almleaky, Y., Benkhaldoun, Z., Magain, P., Morris, B. M., Heng, K., and Queloz, D. (2017). A seven-planet resonant chain in TRAPPIST-1. *Nature Astronomy*, **1**(0129).

Manabe, S. and Strickler, R. (1964). Thermal Equilibrium of the Atmosphere with a Convective Adjustment. *Journal of the Atmospheric Sciences*, **21**, 361–385.

McBride, B. and Gordon, S. (1994). *Computer Program for Calculation of Complex Chemical Equilibrium Compositions and Applications II. Users Manual and Program Description (NASA,*. NASA, National Aeronautics and Space Administration,Washington, D.C. 20546-0001.

Meadows, V. S., Arney, G. N., Schwieterman, E. W., Lustig-Yaeger, J., Lincowski, A. P., Robinson, T., Domagal-Goldman, S. D., Barnes, R. K., Fleming, D. P., Deitrick, R., Luger, R., Driscoll, P. E., Quinn, T. R., and Crisp, D. (2016). The Habitability of Proxima Centauri b: II: Environmental States and Observational Discriminants. *ArXiv e-prints*, (1608.08620).

Miller-Ricci, E. (2008). The Atmospheric Signatures of Super-Earths: How to Distinguish Between Hydrogen-Rich and Hydrogen-Poor Atmospheres. *ApJ*, **690**(2).

Molliere, P., van Boekel, R., Dullemond, C., Henning, T., and Mordasini, C. (2015). Model atmospheres of irradiated exoplanets: the influence of stellar parameters, metallicity, and the C/O ratio. *ApJ*, **813**(47).

Morley, C., Kreidberg, L., Rustamkulov, Z., Robinson, T., and Fortney, J. (2017). Observing the atmospheres of known temperature Earth-sized planets with JWST. *ArXiv e-prints*, **1708.04239v1**.

NASA (1976). US Standard Atmosphere, 1976.

NASA (2017). Kepler and K2, NASA.

O'Malley-James, J. T. and Kaltenegger, L. (2017). Uv surface habitability of the trappist-1 system. *MNRAS*, (1702.06936).

Pierrehumbert, R. (2010). *Principles of Planetary Climate*. Cambridge University Press.

Ramanthan, V. and Coakley Jr., J. (1978). Climate Modeling Through Radiative-Convective Models. *Reviews of Geophysics and Space Physics*, **16**(4).

Rasool, S., Hogan, J., Stewart, R., and Russell, L. (1970). Temperature Distributions in the Lower Atmosphere of Mars from Mariner 6 and 7 Radio Occultation Data. *Journal of the Atmospheric Sciences*, **27**, 841–843.

Rogers, L. (2014). Most 1.6 Earth Radius Planets are not Rocky. *ApJ*, **801**(41).

Rothman, L., Gordon, I., Babikov, Y., Barbe, A., Benner, C., Bernath, P., Birk, M., and et al. (2013). The HITRAN2012 molecular spectroscopic database. *Journal of Quantitative Spectroscopy and Radiative Transfer*, **130**, 4–50.

Schaefer, L. and Fegley Jr., B. (2009). Chemistry of Atmospheres Formed during Accretion of Earth and Other Terrestrial Planets. *Icarus*, **208**(1).

Seager, S. (2010). *Exoplanet Atmospheres: Physical Processes*. Princeton University Press.

Seager, S. and Deming, D. (2010). Exoplanet Atmospheres. *ARAA*, **48**(631).

Southworth, J., Mancini, L., Madhusudhan, N., Mollière, P., Ciceri, S., and Henning, T. (2016). Detection of the atmosphere of the 1.6 Earth mass exoplanet GJ 1132b . *ApJ*, **153**(4).

Tennyson, J., Yurchenko, S. N., Al-Refaie, A. F., Barton, E. J., Chubb, K. L., Coles, P. A., Diamantopoulou, S., Gorman, M. N., Hill, C., Lam, A. Z., Lodi, L., McKemmish, L. K., Na, Y., Owens, A., Polyansky, O. L., Rivlin, T., Sousa-Silva, C., Underwood, D. S., Yachmenev, A., and Zak, E. (2016). The exomol database: Molecular line lists for exoplanet and other hot atmospheres. *Journal of Molecular Spectroscopy*, **327**, 73–94.

Titov, D. V., Bullock, M. A., Crisp, D., Renno, N. O., Taylor, F. W., and Zasova, L. V. (2013). *Radiation in the Atmosphere of Venus*, pages 121–138. American Geophysical Union.

Tsiaras, A., Rocchetto, M., Waldmann, I. P., Venot, O., Varley, R., Morello, G., Damiano, M., Tinetti, G., Barton, E. J., Yurchenko, S. N., and Tennyson, J. (2016). Detection of an atmosphere around the Super-Earth 55 Cancri e. *ApJ*, **820**(99).

Unterborn, C., Desch, S., Hinkel, N., and Lorenzo, A. (2017). Constraining the Compositions of the TRAPPIST-1 Planets to Trace Snow Lines and Migration in M Dwarf Disks. *ArXiv e-prints*, (1706.02689v1).

von Paris, P., Gebauer, S., Godolt, M., Rauer, H., and Stracke, B. (2011). Atmospheric studies of habitability in the Gliese 581 system. *Astronomy and Astrophysics*, **532**(A58).

Wheatley, P., Louden, T., Bourrier, V., Ehrenreich, D., and Gillon, M. (2017). Strong XUV irradiation of the Earth-sized exoplanets orbiting the ultracool dwarf TRAPPIST-1. *MNRAS*, **465**(1).